Ain Shams Engineering Journal 13 (2022) 101592

Contents lists available at ScienceDirect

Ain Shams Engineering Journal

journal homepage: www.sciencedirect.com

Civil Engineering

3D numerical simulation of slope-flexible system interaction using a mixed FEM-SPH model

Jose Carlos Jimenez Fernandez [a], Laura Castanon-Jano [b,*], Alvaro Gaute Alonso [c], Elena Blanco-Fernandez [b], Juan Carlos Gonzalez Fernandez [d], Victor Centeno Gonzalez [d], Daniel Castro-Fresno [b], David Garcia-Sanchez [a]

[a] TECNALIA, Basque Research and Technology Alliance (BRTA), Parque Científico y Tecnológico de Bizkaia, Astondo Bidea Edificio 700, 48160 Derio, Spain
[b] GITECO Research Group, University of Cantabria, 39005 Santander, Spain
[c] Department of Structural Engineering and Mechanics, University of Cantabria, 39005 Santander, Spain
[d] WSP SPAIN - APIA, Parque Científico y Tecnológico de Cantabria (PCTCAN). Av. Albert Einstein, 6, 39011 Santander, Spain

ARTICLE INFO

Article history:
Received 8 June 2021
Revised 17 August 2021
Accepted 22 September 2021
Available online 06 October 2021

Keywords:
Slope protection
Flexible systems
Numerical simulation
FEM
SPH
Soil-structure interaction

ABSTRACT

Flexible membranes are light structures anchored to the ground that protect infrastructures or dwellings from rock or soil sliding. One alternative to design these structures is by using numerical simulations. However, very few models were found until date and most of them are in 2D and do not include all their components. This paper presents the development of a numerical model combining Finite Element Modelling (FEM) with Smooth Particle Hydrodynamics (SPH) formulation. Both cylindrical and spherical failure of the slope were simulated. One reference geometry of the slope was designed and a total of 21 slip circles were calculated considering different soil parameters, phreatic level position and drainage solutions. Four case studies were extracted from these scenarios and simulated using different dimensions of the components of the system. As a validation model, an experimental test that imitates the soil detachment and its retention by the steel membrane was successfully reproduced.

1. Introduction

In the last decades landslides and falling of rocks are becoming more and more common, mainly due to the climate change that is leading to extreme temperatures and heavy rains or droughts [1]. In this context the slope stabilisation and protection systems play a great role, aimed at minimising the damages on roads, railways or towns. The stabilisation and protection measurement implanted in a certain area depends mainly on the volume of the potential sliding material and the type of terrain (soil, rocks, mixed) [2,3]. Examples of these systems are soil nailing, shotcrete, embankments, rockfall barriers or flexible systems anchored to the ground.

Focusing on flexible systems, they are a useful solution when dealing with instabilities, especially effective with those up to 3-meter depth [4]. Flexible systems are also a relatively cheap solution of quick installation [5] when compared with others, like embankments or soil nailing. However, there is a lack of information in the literature related to the design that causes certain distrust in the contractors.

Flexible systems consist of a resistant membrane (cable net or wire mesh) and secondary membranes, installed one after the other that cover the surface to be protected (Fig. 1). Reinforced cables in a square or rhomboidal pattern are used to hold the membranes to the ground. At the intersection of vertical and horizontal cables, a bolt is installed to fix them together with the membranes, using an anchor plate and screw. Perimeter cables are used to close the boundaries of the area to be stabilized. If the main membrane is a strong wire mesh, the use of reinforcement cables is not mandatory but optional.

This work is part of the Foresee project, the general objective of which is to develop and validate a series of tools in order to increase resilience in road and rail corridors, as well as in multimodal terminals, in the face of extreme events such as floods, landslides or earthquakes. For this, technological innovations and other methodologies are developed that will allow to anticipate, adapt and mitigate the negative effects of extreme events on the

* Corresponding author.
E-mail address: laura.castanon@unican.es (L. Castanon-Jano).
Peer review under responsibility of Ain Shams University.

Production and hosting by Elsevier

https://doi.org/10.1016/j.asej.2021.09.019

Fig. 1. Flexible membrane anchored to the ground.

transport network. Here, the use of numerical simulations of flexible systems and their interaction with the soil can be seen clearly as a design tool that has the aim of dimensioning the elements to be installed in the system, thus minimising the consequences of the event.

The design tool presented below is based on the consideration that these systems have a passive behaviour. This means that the systems will work containing the unstable mass once the break has occurred. It was corroborated in [6] and is opposite to most of the design models, which assume that the flexible system is able to avoid the sliding of the ground [7].

The use of numerical simulations using Finite Element Modelling (FEM), Discrete Element Modelling (DEM) or Smooth Particle Hydrodynamics (SPH) has become essential for many design applications in slope protection, such as rockfall barriers [6,8] or embankments for retention of rocks [9,10]. Soil nail walls [11], soldier-piled excavations [12] or braced excavation [13] were also evaluated using FEM, DEM or SPH. Even finite element analysis was used to estimate the slope instability with no protection measurements [14–16]. However, the use of this kind of software in flexible systems is very limited.

The first implementation of a numerical model of a wire mesh anchored to the ground and its use as a design tool was carried out by [17], using ABAQUS software as FEM tool. The main drawback is that the instability and consequent soil movement was not integrated in the model, since the ground was modelled as a plain surface. On the other hand, a methodology based on the use of SPH to represent the behaviour of the soil was demonstrated to be adequate and accurate to predict the break circle [18–20].

Despite the suitability of using mixed FEM-SPH formulations, till date, there is only one work [7] that implements a numerical model using both computational methods: a 2D model in which the FEM membrane interacts with the soil which is discretised by using SPH. Although showing good results, there are some considerations not included in it that would help to more reliably reproduce the geometry and loading conditions of the flexible system, allowing to evaluate more complex cases. Thus, the information of this paper will be used as a starting point and the contribution of the paper will improve the model on the following aspects:

- Incorporation of the depth of unstable soil as a break circle shape, both with cylindrical and spherical failure, instead of a fixed thickness parallel to the slope surface.
- Consideration of different phreatic levels and therefore of dry, submerged or saturated soil.
- Addition of reinforcement cables and perimeter cables in the model (not included in [7]).
- Addition of bolts on the intersections of the reinforcement cables, not as fixed points of limited movement, but as deformable elements with their real length.
- Change from 2D to 3D. This change is mandatory to achieve some of the previous points.

With these new considerations, all the flexible membrane components will be included in the model. Reinforcement cables, perimeter cables and bolts can be dimensioned now besides the other elements that already existed in previous models. In addition, this will avoid an over dimensioning, since the real soil conditions are also input to the software. At last, a personalized solution for each slope problem is achieved. Hence, the main contribution of this work is the model being used as a design tool for the complete structure.

2. Modelisation process

The simulation process is divided in two main phases: i) the determination of the slip circle dimensions, ii) the numerical simulation of the slip circle and flexible system.

For carrying out the first phase, the software SLIDE V7 de Rocscience Inc has been used selecting the Bishop simplified method. The aim of these calculations is to analyse whether a slope is stable or not and, in the cases that might not be stable, calculate the dimensions of the slip circle. At this stage there is no need to consider the flexible system. As discussed in [7], the flexible system will be able to exert some level of force over the soil once that the slip circle has already started its displacement downslope. In Section 4 different scenarios changing the material properties, phreatic level position and drainage interventions in order to calculate 21 different slip circles are presented.

The second phase consists on performing a numerical simulation between a flexible system and unstable slope (Section 5). The flexible system is represented through its main components: membrane, cables and bolts. The unstable slope is represented by a moving mass which is the slip circle. In order to model the large deformations that the slip circle might experience along its falling down the slope, SPH (Smooth Particle Hydrodynamics) has been selected instead of traditional FEM. Besides, membrane, bolts and cables have been discretised with FEM. The software used to model the interaction between flexible system and unstable soil is Autodyn, since it includes both SPH and FEM formulations. The software also allows to model dynamic phenomena with its explicit analysis option, which is an adequate approach to model the impact among soil and membrane. The aim of this simulation is to determine the maximum stresses in the membrane, cables and bolts to adequately dimension the whole system.

In order to model the interaction of flexible system and unstable soil, it has been necessary to define the material properties of membrane, cables and bolts. The membrane (cable net of wire mesh) has been modelled by a continuous shell type element with no bending stiffness. To determine its equivalent Young modulus (or bulk modulus) and poison coefficient (or shear modulus), laboratory test on membranes and cables were performed to obtain those parameters (Section 3). Material properties to model the bolts were obtained directly from commercial Gewi bars technical specifications [21].

3. Experimental testing of components

3.1. Membranes

The membranes analysed here consist of a combination of two layers, each one having different purposes. The main membrane is

made of a cable net fixed with clips in each intersection that has the aim to resist the loads given by the slope. On the contrary, the secondary membrane, installed under the main one, is used with the purpose of closing the big gaps of the cable net pattern and avoid the small rocks and/or soil to trespass the system and achieve the area to be protected, so it does not have a resistant purpose.

The membranes were submitted to a distributed load test (Fig. 2). The net sample is fixed around its perimeter, restricting the three directions of movement, to a steel frame designed for this purpose, trying to make the membrane fit perfectly to it without being slack in order to minimize the initial vertical displacement. The test consists on the application of a perpendicular load, with the help of a press and a square plate on the center of the membrane, which is distributed to the whole area thanks to the use of gravel sacks disposed in a pyramidal shape.

The tests were carried out in the facilities of the Department of Structural Engineering of the University of Cantabria, taking advantage of two vertical beam structures distanced enough that hold a horizontal reinforced beam, in whose centre the press is located. Between the vertical beam structures the test frame was installed. This frame was borrowed by the company Malla Talud Cantabria (MTC), which also were responsible of sewing the cable nets to be tested. The square frame has the following dimensions:

- Inner: 2 m $\times$ 2.3 m
- Outer: 2.35 m $\times$ 2.5 m
- Height: 0.8 m

In this frame, cable nets with two different pattern sizes were tested: square reticule of 300 mm side and square reticule 200 mm side. This was possible due to the versatility of the frame. To accomplish it, the bolts that bear the perimeter reticules can be moved and pinned in different positions, so that the bolts for the 200 mm reticule must be located in the holes with a distance of 282 mm and the bolts for the 300 mm reticule must be inserted in the holes distanced 424 mm. Three tests were carried out for each reticule size. Results can be seen in Fig. 3.

It can be seen that an increment of 100 mm on the reticule side means a reduction of 28% in the maximum load. Looking at Fig. 13, the correlation of the resistance with respect to the net mass is clear: when the load is divided by the mass of each membrane, the curves of the two different reticule sizes (black for the reticule size of 200 mm and green for 300 mm) overlap and follow the same path. With respect to the vertical deflection, it becomes slightly higher (8%) with the increase of the reticule side. Hence, the membrane of 300 mm is, on average, slightly less rigid (more deflection) and also less resistant (lower load). Concerning the progressive increase of slope of the curves, it is coherent with other works like [22], where two main phases are found: the first one with less slope (from 0 mm to around 200–250 mm) corresponding to the adaptation of the sacks to the net, and a second one with a smoother and quasilinear behaviour until reaching the ultimate load. The curves represented here start in a point different from zero due to the fact that the sacks are deposited over the net previous to the application of the load, so at the beginning of the test, the net is under a load equivalent to the weight of the sacks. An

Fig. 2. a) Configuration of the distributed load test, and b) Geometry and connection of the two layers of the membrane, composed by a cable net and a coconut fibre mesh.

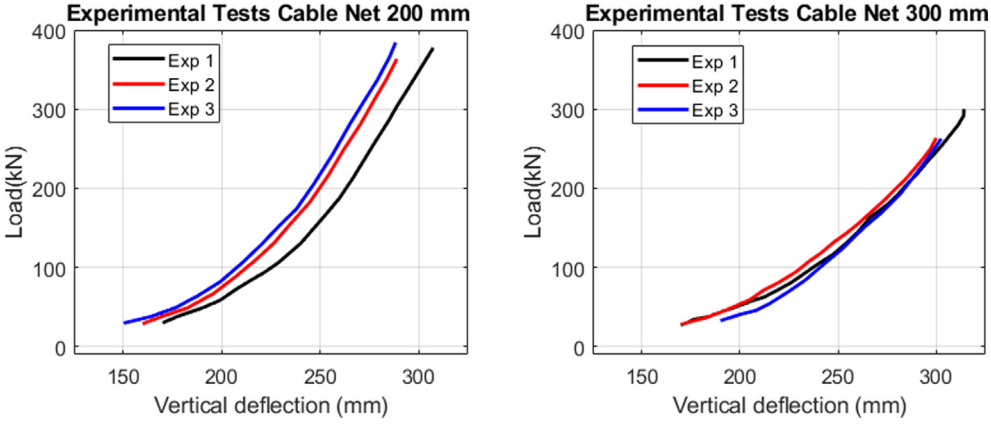

Fig. 3. Load-deflection curves of the cable net of 200 mm reticule with the coconut fibre mesh (left) and of the cable net of 300 mm reticule with the coconut fibre mesh (right).

approximately linear curve from zero to the beginning of the curves could be drawn to represent the whole loading process until breakage, but in this paper only the test curves are shown.

3.2. Cables

The steel cables tested were supplied by the company Malla Talud Cantabria. A total of 6 samples, 16 mm diameter and 680 mm length, were tested at a rate of 0.1 mm/s (test under control of displacements). The tests were done in a Universal Instron 8500 testing machine.

In Fig. 4 the samples after the test are shown. In all cases, one or more strands broke, except in case 3, where the cable broke completely.

The energies absorbed by all the cables are similar (area under the load–displacement curve). The only energy outlier occurs in cable 1, where an early breakage occurs, possibly due to some of its wires being damaged.

Additionally, due lack of availability, only one sample of the 22 mm diameter cable was tested (Fig. 5). The results seem to be rational and coherent with respect to the ones of the 16 mm diameter cable, so it was accepted to be used later to create the numerical model.

4. Slip circle scenarios

An ample set of scenarios are analysed, creating different slope failure simulation cases when the solution kit is complemented by different drainage setups. The possible combinations of soil failure stability analyses considering variations in strength parameters, water table position and slope geometry are very high.

In order to delimit the problem to a practical solution that provides breaks similar to those observed in real cases, the following situations have been established:

- 3 positions of the water table (dry slope, slope with intermediate water table and completely saturated soil)
- 3 types of soils have been considered, which represent most of the usual situations in the study of slope stability (low, medium and high resistance).
- Slope fixed geometry to obtain the different safety factor only in changed condition in water table or soil strength.
- 2D calculation with Slide V7 Rocscience Inc.

Other assumptions (i.e. 3D calculation or variable geometry) would lead to cases that are more complicated to solve but with very similar results and would not add value to the conclusions drawn from the analysis performed.

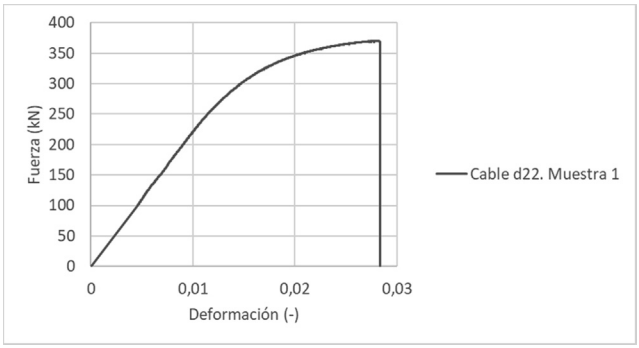

Fig. 5. Load-displacement curve of 22 mm diameter cable.

With those combinations 21 different cases are possible and have been analysed.

4.1. Water table scenarios

The position of the water table with respect to the slope geometry is the first parameter considered to create different situations. The scenarios can be characterized based on their saturation level, with the purpose of achieving the desired FORESEE Smart Slope Stabilization Protection System. The saturation scenario levels are divided in the next situations:

- High Saturated soil with water level at the top of the excavation.
- Medium saturated soil (water table lowering towards the edge of the slope)
- Low saturated soil with water level at the top of the slope.

4.2. Geotechnical soil parameters

The composition of the soil is the second variable parameter considered to create the FORESEE Slope Stabilization-Protection Drainage Scenarios. The main soil composition types considered for the analysis are based on the observation and experience. The choice of geotechnical properties is based on the usual soil parameters obtained from experience, considering a variation of 6° in the angle of internal friction between the least resistant and the most resistant.

- Low resistance soils without cementation
  - o Cohesion 20 kPa
  - o Friction 26°
  - o Unit weight 18 kN/m^3
  - o Saturated unit weight 20kN/m^3
- Medium resistance soil

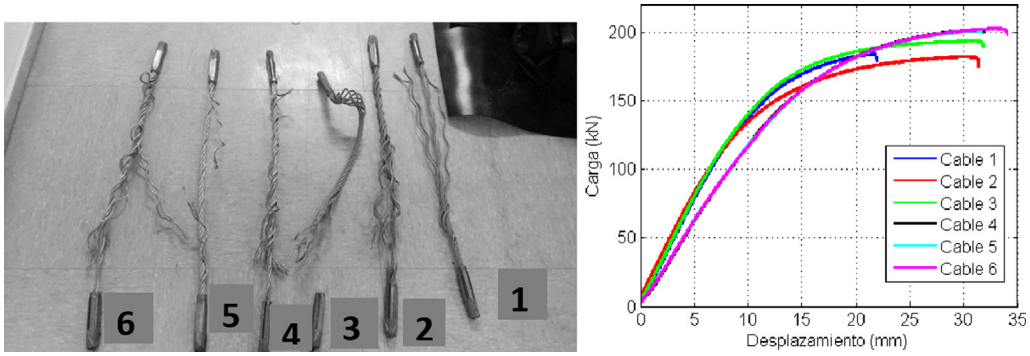

Fig. 4. Appearance of 16 mm diameter cables after performing the tension tests and Load-displacement curves.

- o Cohesion 20 kPa
- o Friction 32°
- o Unit weight 18 kN/m^3
- o Saturated unit weight 20kN/m^3
- • High strength or lightly cemented soil
- o Cohesion 20 kPa
- o Friction 36°
- o Unit weight 18 kN/m^3
- o Saturated unit weight 20kN/m^3

The last model of soil, 'High strength or lightly cemented soil' qualifies to represent hard geological materials that cannot be considered a rock according to the definition of ISRM (International Society for Rock Mechanics and Rock Engineering) but still, are much harder than a typical soil. An example of these type of hard soils are the 'jabres', which come from the weathering of granitic rocks and that still maintain a certain degree of cementation of the original rock. Another example are the sands and clays partially cemented from the Cretaceous-Tertiary. In both cases, these particular cemented soils are considered as standard soils in typical geotechnical design problems, like slope stability analyses and bearing capacity in foundations.

4.3. Geometry and slope parameters

Apart from the main water table and soil type characteristics, the scenarios are defined to force circular breaks with a geometry and dimensions approximating those observed in the breaks produced in several real slopes studied along our professional experience. Therefore, the following angle and height have been chosen to simplify the cases to avoid the infinite number come from combining cases of different slope, water table and height.

- Slope geometry: angle 56° (2H/3V) and height between 10 and 15 m (i.e. 13,26 m) (Fig. 6).

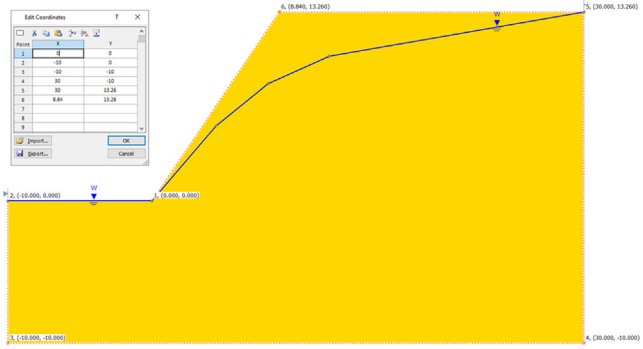

Fig. 6. Slope model created in "Slide V7, Rocscience Limit Equilibrium Slope Stability".

The boundary model coordinates used for the calculation are shown in the next figure, defining the extents of the soil region to analyse, extracted from the Slide V7 (Rocscience Limit Equilibrium Slope Stability software):

4.4. Methodology and scenarios selected

Twenty-one scenarios have been analysed. The first nine scenarios are created to describe a wide reference base-case of possible water table levels and soil types that might be representative of the majority of cases of interest. These cases were selected based on the balance between the wide scope purposes and the usefulness to the development of the new Slope Stabilization-Protection Systems. The following twelve cases have the same geometric conditions and water level as those previously mentioned, complementing these with different drainage solutions.

4.5. Simulations and calculations

The Bishop Simplified vertical slice limit equilibrium method has been chosen to calculate slope stability and potential failure geometry. The methodology used, safety factor (SF) and conditions are described in [13], and was calculated using "*Slide V7, Rocscience limit equilibrium slope stability*" software, using all the parameters defined previously. In order to reduce the computing-time calculation, a two-dimensional approach was selected considering plane-strain conditions.

The summary of the cases is presented in Table 1, Table 2 and Table 3, including the safety factor (SF) related to each scenario.

4.6. Descriptions of cases and failure curves

The drainage characteristics for the 21 cases are:

- Cases 1–4-7 would correspond to complete saturation of the slope and without drainage actions.
- Cases 2–5-8 of intermediate water in the slope conform to what would be obtained in cases 10–13-16, that is, with a 1 m deep head drain, usual in the practice, filling with a draining material, evacuating water in a longitudinal direction up to the exit of the slope with the natural slope. These breaks coincide in shape and safety factor. The safety factor is not exact because the properties of the drainage ditch to assess the water pressure have been changed.
- Cases 3–6-9 with long-term depressed water table by excavation and cases 11–14-17 with horizontal drilled hole (horizontal drains) approximately ½ the height of the slope (6 m in the model) give rise to breaks with safety factors and shapes almost identical to "naturally" drained slope cases.

Table 1
Reference Slope Scenarios based on water table levels and soil type.

Safety Factor (SF)		Groundwater level position		
		High water table	Intermediate water table	Low water table
Soil type	Soil low resistance	Case 1	Case 2	Case 3
	Soil medium resistance	Case 4	Case 5	Case 6
	Soil high resistance	Case 7	Case 8	Case 9
SAFETY FACTOR SLIDE V7. BISHOP SIMPLIFIED METHOD		Groundwater level position SF High water table	SF intermediate water table	SS low water table
Soil type	Soil low resistance	0.547	0.825	1.110
	Soil medium resistance	0.566	0.912	1.268
	Soil high resistance	0.577	0.977	1.382

Table 2
Slope Scenarios with added drainage solutions (Drilled holes and slope head trench).

Safety Factor (SF)		Groundwater level position		
		High water table	Intermediate water table	Low water table
Soil type	Soil low resistance	Case 10	Case 11	Case 12
	Soil medium resistance	Case 13	Case 14	Case 15
	Soil high resistance	Case 16	Case 17	Case 18
SAFETY FACTOR SLIDE V7. BISHOP SIMPLIFIED METHOD		Groundwater level position		
		SF High water table	SF intermediate water table	SS low water table
Soil type	Soil low resistance	0.856	1.119	1.118
	Soil medium resistance	0.945	1.278	1.276
	Soil high resistance	1.009	1.390	1.387

Table 3
Additional Slope Scenarios with added drainage solutions.

Safety factor (SF)		Groundwater level position-with drainage actions
		Drilled holds in slope face. Water level intermediate/low position
Soil type	Soil low resistance	Case 19
	Soil medium resistance	Case 20
	Soil high resistance	Case 21
SAFETY FACTOR SLIDE V7. BISHOP SIMPLIFIED METHOD		Groundwater level position-with drainage actions
		Drilled holds in slope face. Water level intermediate/low position
Soil type	Soil low resistance	1.119
	Soil medium resistance	1.278
	Soil high resistance	1.390

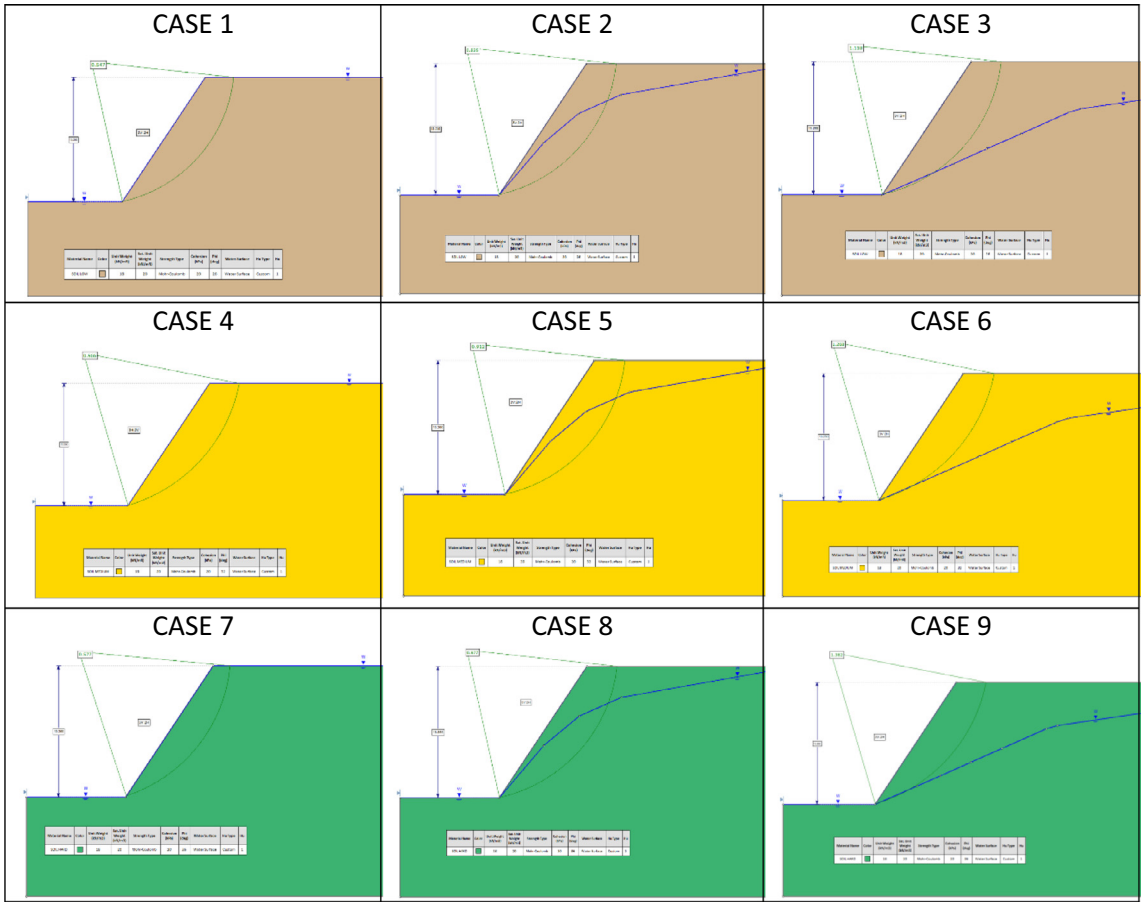

Fig. 7. Slope models for reference scenarios without drainage elements (cases 1–9).

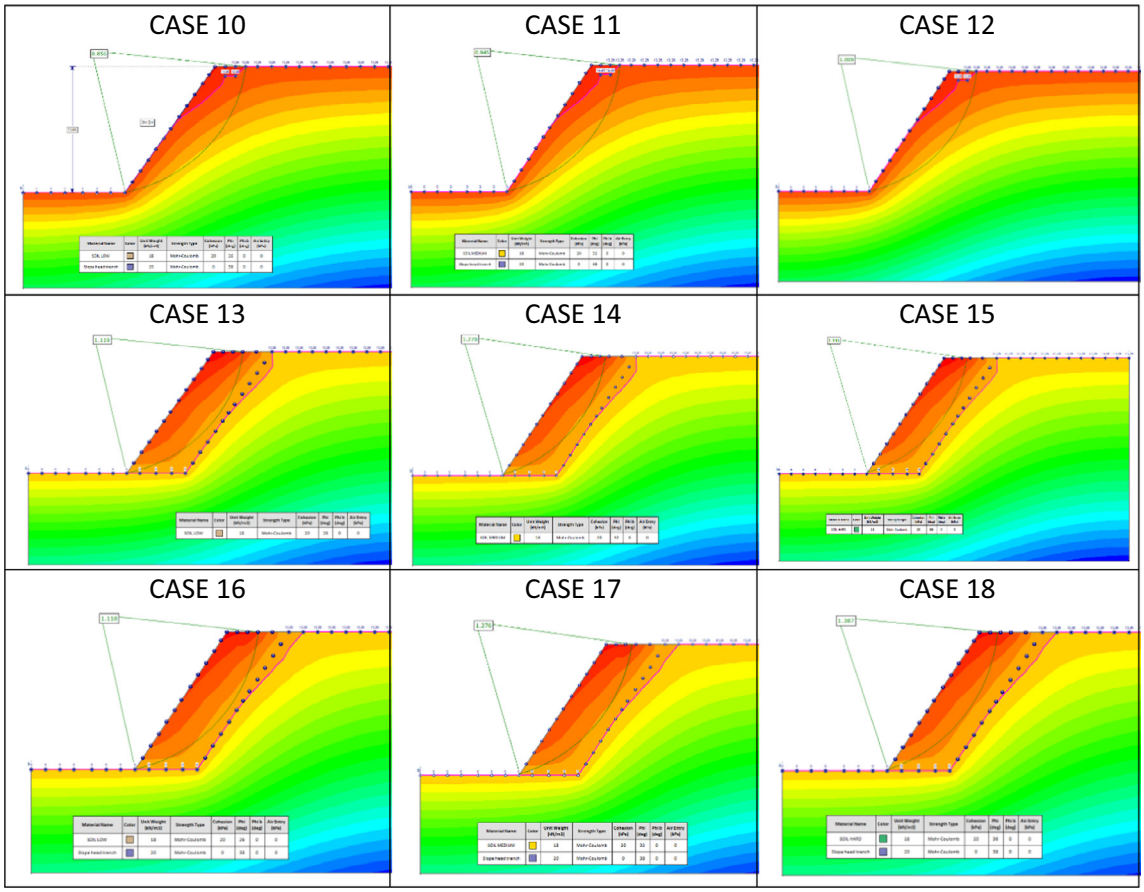

Fig. 8. Slope models for reference scenarios with drainage elements (cases 10–18).

- Cases 12–15-18 with slope head trench and horizontal drains of approximately ½ the height of the slope entail the same result and form of failure, considering only deep drainage with drains, with minimal differences to the properties of the cited drainage ditch.
- Finally, cases 19–20-21 of horizontal drains of approximately ½ the height of the slope entail the same result and form of failure, considering only deep drainage with drains, and a medium water level position.

Fig. 7 shows the different cases without drainage solutions including potential failure curves and their safety factors (SF):

Fig. 8 shows the different cases with drainage solutions including potential failure curves and their safety factors (SF):

The additional models (cases 19 – 21) with drainage solutions (drilled hole in slope face) with water level intermediate / low position are shown in Fig. 9.

Four cases of all of the represented here will be selected and implemented on the numerical SPH-FEM models of Section 6 to evaluate the resistance of the slope protection systems.

5. Numerical modelling of soil-flexible system interaction

The numerical simulations of the flexible systems were carried out using Autodyn software, that deals with the resolution of dynamic problems involving impacts, severe loads in a short duration and large deformation (or even failure) of materials. It can be used directly as a resolution engine in the module "Explicit

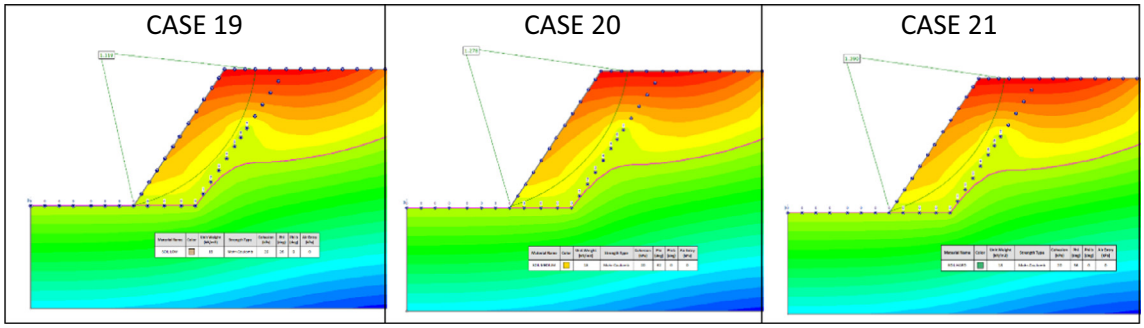

Fig. 9. Slope models for reference scenarios with drainage elements (cases 19–21).

Dynamics" of Ansys Workbench, in case only solids mechanics are simulated, but it also has its own independent module with its own interface, especially suitable to combine solids with the computational method of Smooth Particle Hydrodynamics (SPH).

5.1. Soil

Soil was simulated using SPH, as it was probed to work adequately in reproducing the slope failure and post-failure [7,23,24].

The material properties of the soil were implemented by choosing the SAND model from the material library of Autodyn. The Equation of State (EOS) is Compaction Linear, which has demonstrated a good approach to simulate granular materials [25]. The values introduced for the sand material are extracted from the studies of [26]. It must be noted that at the time of calculating the different case studies (discussed in Section 6) the soil densities are different from the values shown in this section (extracted from the software database). To obtain the different values of the material properties being these the most realistic possible, the values employed for the calculations on the case studies have been adapted according to a function that adjusts the curves shapes given by the database for any density dependent variable shown in the paper.

5.2. Components of the flexible system

5.2.1. Membranes

Ideally, to model the membrane with the geometry most similar to the reality, each of its cables should be introduced as lines, given truss behaviour (no flexural rigidity) and the stress–strain properties of the cables should be added. However, due to the large extension of the areas to be protected (and hence implemented on the software) the computational time would be unaffordable. Having this into account, a simplification of the cable nets must be done: the membrane that covers the slope is numerically simplified using shell elements, instead of simulating each cable using linear elements. For all this, the first step consists of finding out the properties of a shell that behaves in an equivalent way to the cable net. To do this, the load–displacement results of the uniformly distributed load tests were used as reference curves to be pursued by the equivalent shell model. The module of Ansys Workbench used to achieve this simplification was the called "Explicit Dynamic" which uses the resolution engine Autodyn. This was done due to two facts: 1) only solids are included, and 2) the much friendlier interface. The properties obtained for each membrane are then introduced in the module Autodyn when implementing the more complex model of flexible membrane interacting with an SPH based soil (Sections 5.4, 5.5 and 6).

The membrane model is initially built as follows: a surface of dimensions 2 m by 2.3 m was created, the same dimensions as the internal square of the steel frame in which the experimental tests were carried out. A thickness of 1 mm was given to the surface to reduce its bending stiffness and approximate it to a membrane. The four sides of the surface were constrained, limiting their displacement to zero in x, y and z directions. A solid with the geometry of the final deformed state of membrane was created, and a linear displacement is applied to it in direction to the membrane. A zero-friction coefficient is given to the interaction between the solid and the membrane. The initial conditions can be seen in Fig. 10.

The mesh size was 250 mm. The material assigned to the surface only includes three basic properties: density, Young modulus and Poisson coefficient.

The Young modulus was calculated by iterating it until obtaining a Load-Displacement curve that matches the experimental ones. The first cable net simulated and adjusted to the experimental results was the 200 mm reticle (Fig. 11). After several iterations it was found that for 1 mm thick, the Young Modulus that best fits is 2000 MPa.

Once the properties of the shell are found, the failure of the shell must be identified somehow. Considering that the model is a sim-

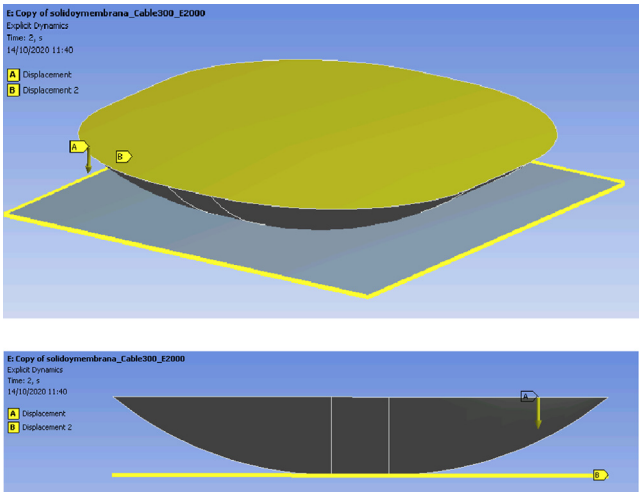

Fig. 10. Geometry of the membrane (2 m x2.3 m) and the solid from which the vertical load is applied.

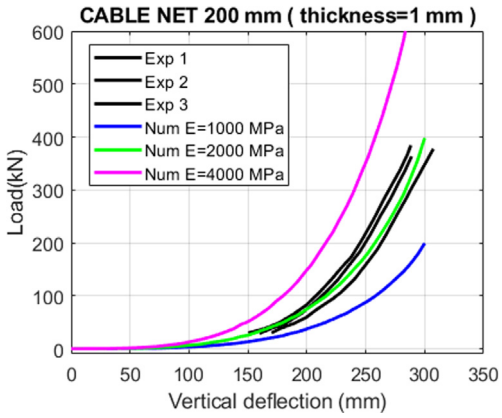

Fig. 11. Experimental and numerical load–deflection curves of the cable net of 200 mm reticle.

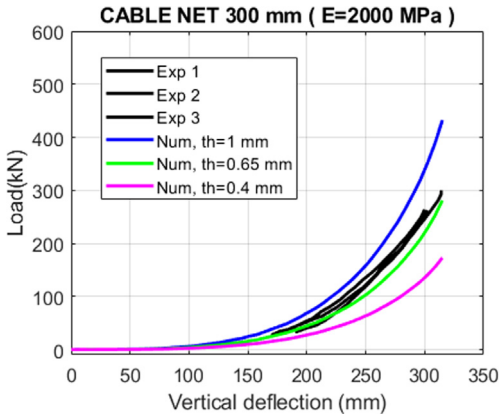

Fig. 12. Experimental and numerical load–deflection curves of the cable net of 300 mm reticle.

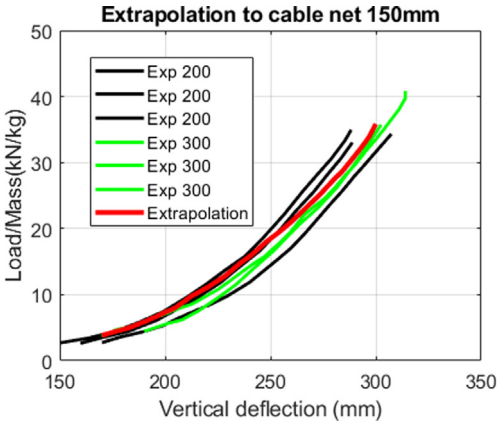

Fig. 13. F/mass vs. vertical displacement for several cable nets.

plification and only elastic (and no plastic) material properties are included, the failure point was detected by means of the maximum Von Misses stress on the maximum deflection of the curve. For a cable net of 200 mm, a Von Misses stress of 150.65 MPa was identified to be the failure limit, to be used in further and more complex simulations of a complete flexible system. Once the cable net of 200 mm is successfully modelled, the one of the cable net of 300 mm of reticle is calibrated by keeping the density and elastic modulus constant and varying its thickness (Fig. 12).

Lastly, a more refined reticule was included in case of heavy landslides impossible to retain with the previous cable nets. That is why a square net of reticle 150 mm was also simulated, although there is no selling of these net geometries yet in the market. Since there is not information about the load–displacement behaviour of cable nets with 150 mm of reticule, an extrapolation was carried out.

Experimental curves of cable nets of 200 mm reticule and 300 mm reticule were represented in the same graph (Fig. 13), in which the x axis represents the vertical displacement and the y axis is the force divided by the mass of the membrane of 2 × 2.3 m. It can be seen that the dispersion among all curves is very low, which means that there is a clear relationship between the mass of a net and its resistance. Thus, one of the curves, specifically one from a 300 mm reticle net, was used to extrapolate the results to one of 150 mm reticle, just by multiplying the y axis by the mass of the new net (Fig. 14).

Then, the same procedure than for cable net of 300 mm was followed to obtain the equivalent properties (thickness) when simulating it as a continuous shell, which is shown in Fig. 14.

Table 4 sums up the properties of the 3 membranes equivalent to the cable nets obtained before.

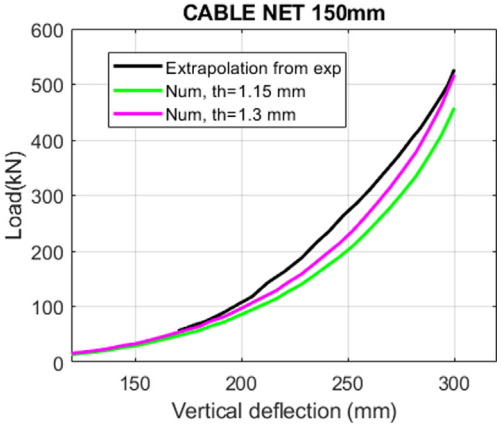

Fig. 14. Experimental (extrapolated) and numerical load–deflection curves of the cable net of 150 mm reticule.

Table 4
Properties of the three membranes equivalent to the cable nets.

	CABLE NET 300 MM	CABLE NET 200 MM	CABLE NET 150 MM
Thickness (mm)	0.65	1	1.3
E (MPa)	2000	2000	2000
v	0.3	0.3	0.3
σ_{VM}(MPa)	168.5	150.65	150.73
F_{max}(kN)	281	378.83	491.84

5.2.2. Cables

Two types of cables have been used in the case studies: Ø16mm and Ø22mm. Mechanical parameters of these elements to be introduced in the model have been obtained from tensile tests made in laboratory (Section 3.2), and from these the yield stress and the ultimate stress are obtained. A perfect elastoplastic behaviour, like the shown in Fig. 15, has been implemented in the models [27] in order to establish the yield stress as the limiting value for the flexible systems considering that their mechanical parameters obtained in Table 4 have been obtained via an elastic approach.

Yield stress for 0.2% of deformation is obtained which is the input for the Von Mises strength criteria (ultimate stress is not represented into the models as it has been said before, as the mechanical behaviour is perfect elastoplastic), and these values are introduced in the material properties in Autodyn software. The material EOS for the cables is Linear and the Bulk modulus is considered instead of the Young modulus, which are related with the Poisson's ratio. Same approach is used to obtain the shear modulus.

Values obtained for each cable diameter are included in Table 5.

5.2.3. Bolts

To obtain the mechanical parameters needed for the simulation of the bolts that are fixed to the flexible system, a data table from a known supplier (DYWIDAG) is employed to get the data for differ-

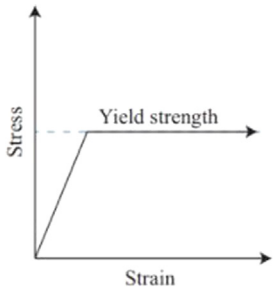

Fig. 15. Perfect elastoplastic behaviour.

Table 5
Stress and strain values of the 16 mm and 22 mm diameter cables.

	Cable 16 mm	Cable 22 mm
σ_{VM}(MPa)	745	920
ε_{VM}(-)	0.0035	0.0043

Table 6
Stress and strain values of the 25 mm and 28 mm diameter bolts (GEWI B500B & S555/700).

Nominal diameter (mm)	Yield stress (MPa)	Ultimate stress (MPa)	Load at the yield stress (kN)	Load at the ultimate stress (kN)	Section (mm^2)
25	500	550	245	270	491
28	500	550	308	339	616

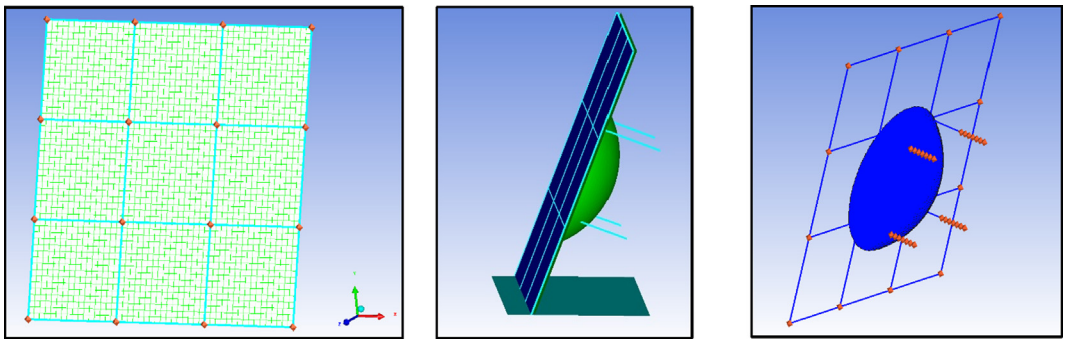

Fig. 16. Model geometry of circular failure, front and side view and last with cables and anchorages, showing the back-sliding surface.

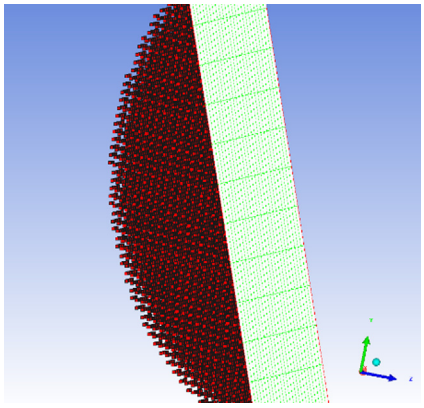

Fig. 17. SPH particles contained between the sliding surface and the flexible system.

ent diameter bolts (Table 6). The anchorages were defined as beam elements, with a truss behaviour as only the pullout force is considered in this study. As for the cables, a perfect elastoplastic behaviour has been adopted in order to consider yield stress as limiting criteria of the models.

No erosion criteria are applied for both cables and bolts, as the target of the simulation is to analyse in the flexible system if the yield stress is reached in any of the cases and elements that will be studied.

5.3. Interactions

Modelisation of three interfaces are needed in the model:

a. mass of soil stable – mass of soil unstable
b. mass of soil unstable – flexible system
c. flexible system – mass of soil stable

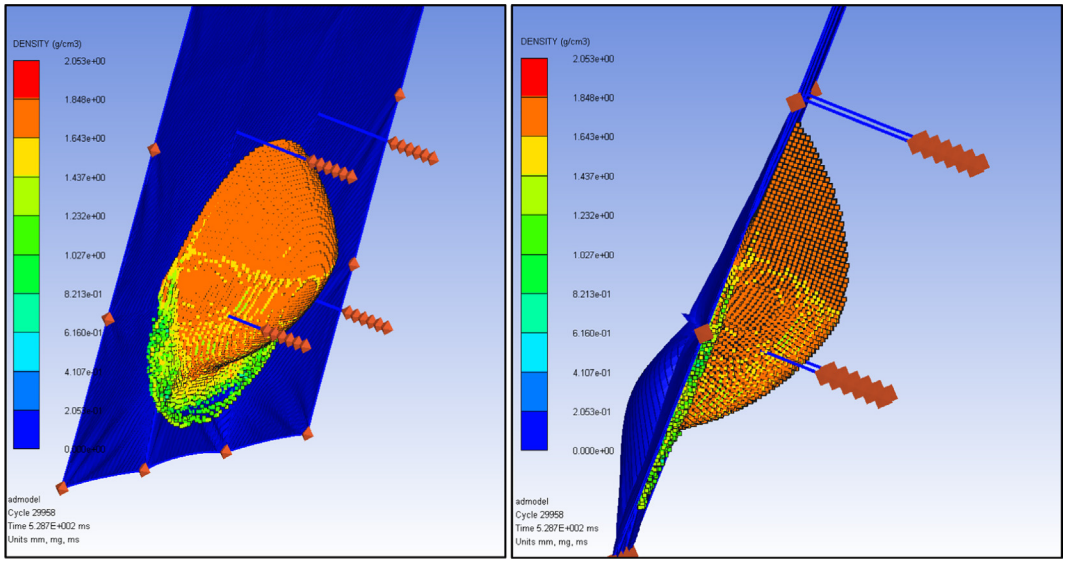

Fig. 18. Density compaction at SPH particles.

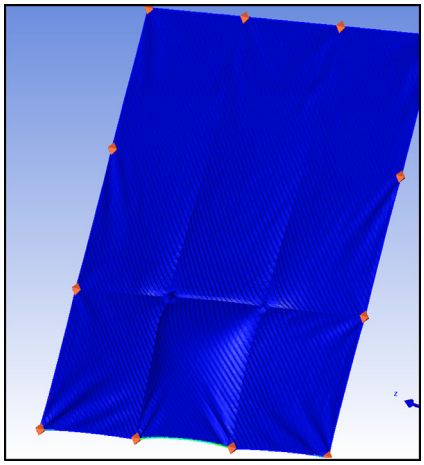

Fig. 19. Deformed flexible system.

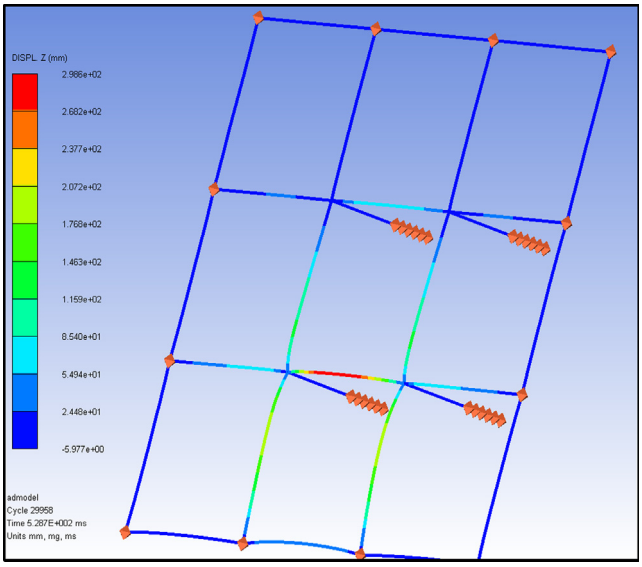

Fig. 20. Perpendicular displacement of cables to the membrane.

The three interfaces are defined as a contact interaction with frictional static coefficients, with different values between each one. This interaction is defined as a Lagrange/Lagrange process, because the SPH formulation is considered a Lagrange body. The defined method is by external gap, where the gap size is automatically calculated and controlled for all the elements that are interacting.

First, the SPH particles will slide along the failure surface and in this case the friction generated will be a residual frictional coefficient. More details of the interaction between mass of soil stable and mass of soil unstable are given on Section 6.2, since it depends on the specific values of the case study considered.

Secondly, the soil wedge will interact with the membrane when this one is retained. Muhunthan et al. 2005 [28] suggested friction angles between soil and mesh between 25° and 60°. Blanco-Fernandez et al., 2011 [4] suggested to adopt as a friction coefficient 0.2 based on considering the lowest friction angle recommended by Muhunthan [28] and divided by 2 the tangent of the angle to be in the safety side. Therefore, friction coefficient between soil and mesh is taken as tan 25°/2 ≈ 0.2. It is assumed that the lower the friction coefficient between the membrane and the soil, the larger the impact force, and therefore, the higher the tensile stresses in the membrane.

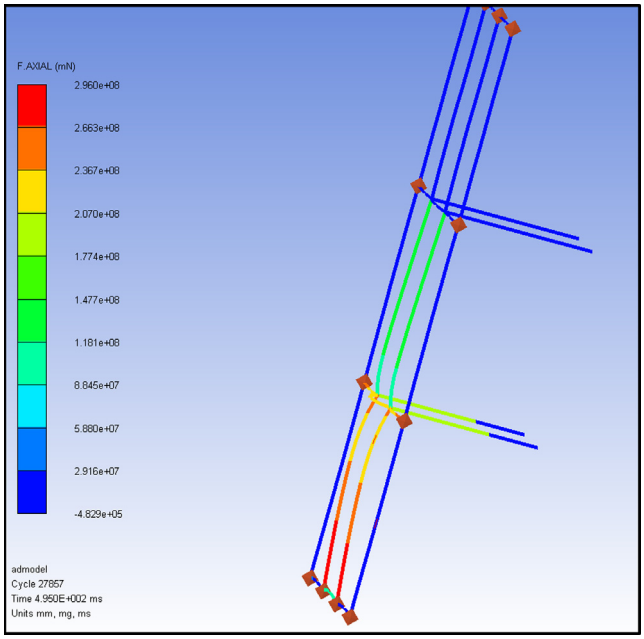

Fig. 21. Axial force of cables.

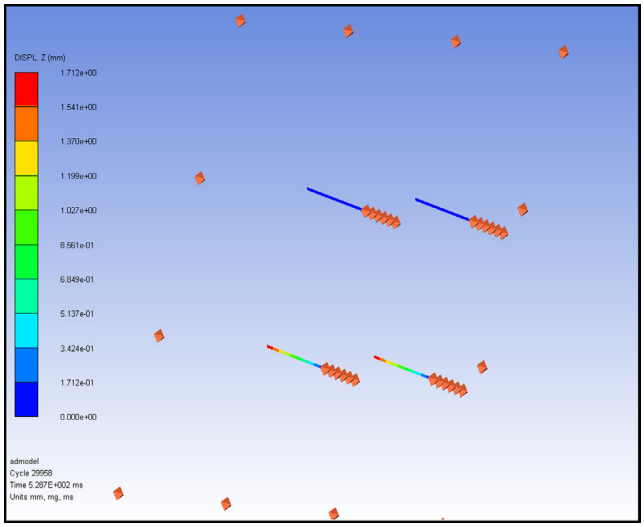

Fig. 22. Longitudinal displacement of bolts.

Finally, the membrane will interact with the surface of sliding at the sides where no SPH particles will be allowed. For simplicity, 0.2 is taken similar to the wedge – membrane case. The sliding surface is fixed, as no movements are expected in this body.

No interaction is defined between the cables and the anchorages with the rest of elements present in the model, but these are going to be linked to the flexible systems through pinned joins (cable and membrane) and rigid joins (anchorage head and membrane). The anchorages are constrained in the other end in several nodes as fixed (no translation or rotation), emulating the grouting or fixing to the rigid part of the soil.

5.4. Model set-up in 3D (spherical failure)

In this first model, the sliding surface of the falling wedge is a cut portion of a sphere generating a circular failure, so the soil material which is going to fall is confined between the sliding surface and the flexible system. The geometry has been designed

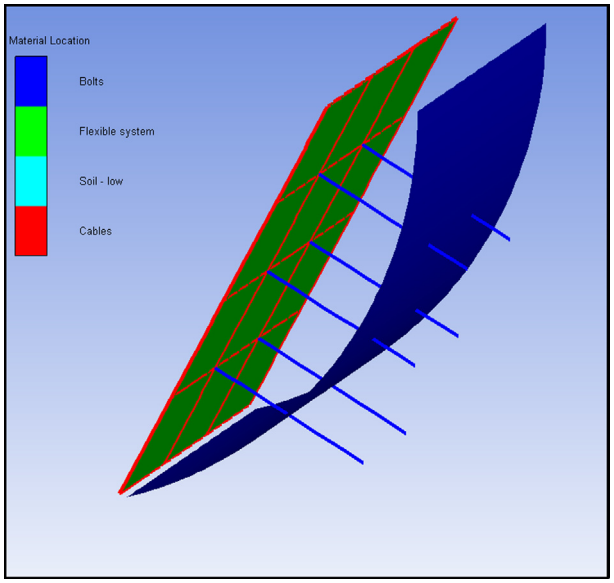

Fig. 23. Autodyn model, general geometry.

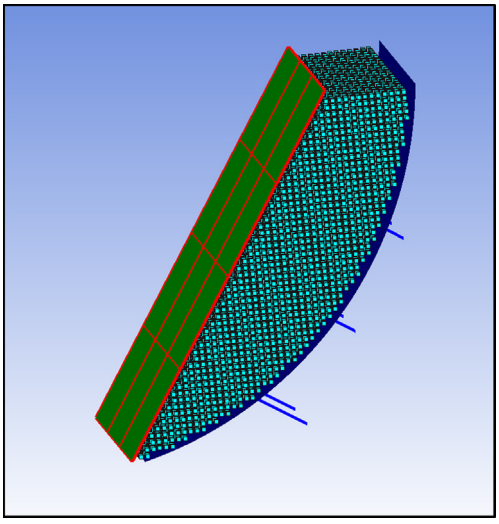

Fig. 26. Model geometry employing a SPH soil wedge with the weighed density.

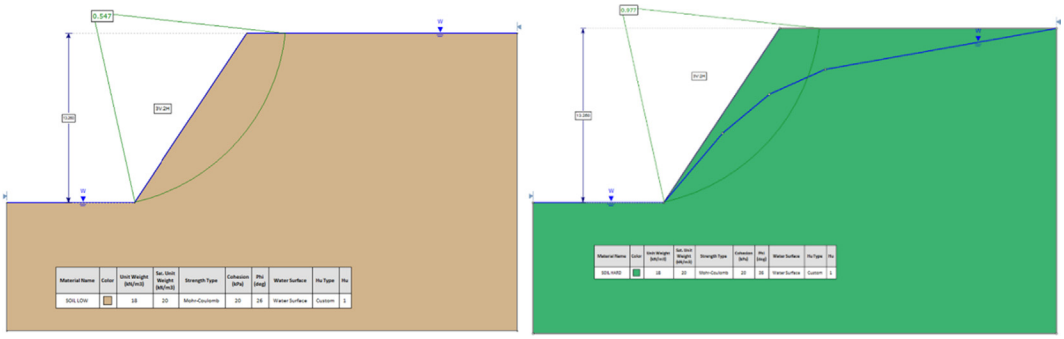

Fig. 24. Geometry, break circle and phreatic level (in blue) of planar cases A and B (left) and planar cases C and D (right).

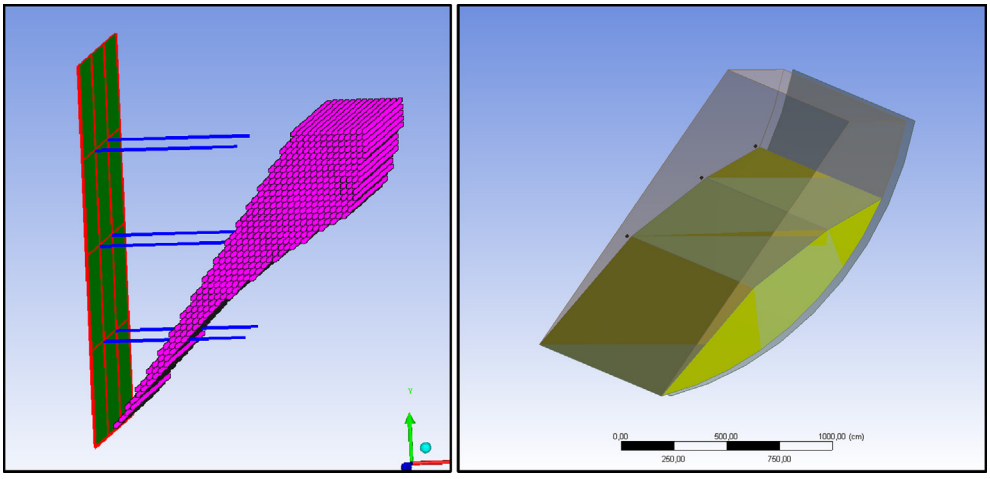

Fig. 25. Left: Dry density volume as SPH, not allowing the software to define an additional SPH volume below to represent the submerged/saturated soil. Right: Modelling of the free-falling soil wedge, with the submerged/saturated volume highlighted.

using the module Geometry Designer in ANSYS Workbench, and after a first preparation of the model through this software, is exported to be used in AUTODYN.

The dimension of the flexible system is 12 × 12 meters, and the bolts are going to be placed in a square distribution of 4 × 4 meters, as it can be seen in the following figure. The inclination of the slope is 20° with respect to the vertical. The model can be seen in Fig. 16.

SPH particles are specified through the sand material previously defined, with an element size appropriate (100 mm) for this model in order to improve the computational cost of the model (see Fig. 17).

As we defined the SPH particles as a granular material, the density variation of these can be evaluated as internal pressure is developed, showing the lower density as the particles have fallen through the sliding surface and are separated from the wedge mass (Fig. 18).

The combined behaviour of the membrane and the cables show the collaboration of these elements adding rigidity to the flexible system as it can be seen in Fig. 19.

Views of the cable-anchorage elements are isolated from the other elements of the model for clarity of visualization (Fig. 20, Fig. 21 and Fig. 22). Interesting values for these elements are the perpendicular displacement to the membrane and the axial force is developed. It can be seen that in the peak of the mass falling, the maximum registered displacement is 300 mm, with axial forces in the cables of around 300 KN, and around 100 KN in the anchorages.

The solution of the spherical failure model confirms the feasibility of an analysis and calculation of flexible slope protection systems when knowing the real extension of the slope detachment. However, in this paper we will only focus on the cylindrical failure (explained in the next subsection), since the slip circles from which the case studies are made are obtained from a 2D software that does not provide the length and the change in depth of the loose material.

5.5. Model set-up in 3D (cylindrical failure)

The process of modelling follows the same steps than explained in the previous cases, so only the differences applied will be presented here.

The flexible system is composed by a cable net and geomembrane of 16 m height by 12 m width. This dimension of the slope is the defined dimension of the slip circle scenarios of section 4 of this paper. The height of the membrane, when rotated to the angle of the slope, will cover its entire length. A 4 × 4 m cable square pattern is modelled for all the scenarios to be analysed, plus 3 rows of bolts at the central portion of the flexible system, fixed at their ends simulating the grouting in the ground (Fig. 23).

Boundary conditions applied to these models follow the same considerations than those taken for the spherical breakage simulations, with fixed perimetric bolts, modelled central anchorages and reinforcement cables. To avoid SPH particles moving to the transversal direction of the model, a transversal boundary condition of no displacement is applied to the SPH particles.

Results obtained with cylindrical failure slopes are shown in Section 7, where a comparative of 4 different cases is exposed. In those, the elements employed have varied according to the results obtained.

6. Case studies

6.1. Slip circles selection

Four different cases (A, B, C, D) have been selected to be modelled using SPH based on the 21 slip circles simulated in Section 4. Case A and Case B geometry correspond to the Case 1 (no drainage interventions, soil low resistance, high water level, Fig. 24 left). As it can be seen in Table 1, Case 1 presents the lowest SF among the 9 scenarios without any kind of drainage intervention. Case C and Case D correspond to Case 8 (no drainage interventions, soil high resistance, intermediate water level) which has the highest SF among those below 1.0. In case A and case C, submerged soil density (γ_{sum}) has been considered for the soil under the phreatic level while in case B and D saturated soil density (γ_{sat}) was chosen instead.

The reason why two variations of density, γ_{sum} and γ_{sat}, are considered is because Autodyn is not able to deal with pore water pressures and thus, work with effective stresses. Since it was unclear which one of these two densities might provoke the highest tensile stress on the membrane, extreme values such as γ_{sum} and γ_{sat} were taken.

In Case C and D, since the phreatic level divides the slip circle in two sections (see Fig. 24 right), a weighed density has been considered based on γ_{sum} and γ_{sat} and the surface of the slip circle that each density occupies.

Autodyn software does not allow to introduce the effect of the soil cohesion, so this lack of parameters can be relatively covered

Table 7
Summary of the properties of each case study.

	Case A	Case B	Case C	Case D
Phreatic level	Fig. 24 LEFT	Fig. 24 LEFT	Fig. 24 RIGHT	Fig. 24 RIGHT
Slip circle	Cylindrical	Cylindrical	Cylindrical	Cylindrical
Soil characteristics	Low: -Cohesion 20 kPa -Friction 26° -Unit weight 18 kN/m^3 -Saturated unit weight 20kN/m^3	Low: -Cohesion 20 kPa -Friction 26°-Unit weight 18 kN/m^3 -Saturated unit weight 20kN/m^3	High: -Cohesion 20 kPa -Friction 36° -Unit weight 18 kN/m^3 -Saturated unit weight 20kN/m^3	High: -Cohesion 20 kPa -Friction 36° -Unit weight 18 kN/m^3 -Saturated unit weight 20kN/m^3
Soil density	Submerged density: 1.019 g/cm^3	Saturated density: 2.03 g/cm^3	Submerged density: 1.09 g/cm^3 Dry density: 1.836 g/cm^3	Saturated density: 2.03 g/cm^3 Dry density: 1.836 g/cm^3
Friction soil-sliding surface	μd = 0.44	μd = 0.44	μd = tg (Φres) = 0.67	μd = tg (Φres) = 0.67
Cable net	200 mm	200 mm	150 mm	150 mm
Reinforcement and perimeter cables	16 mm	16 mm	16 mm	22 mm
Bolts	28 mm	28 mm	28 mm	28 mm

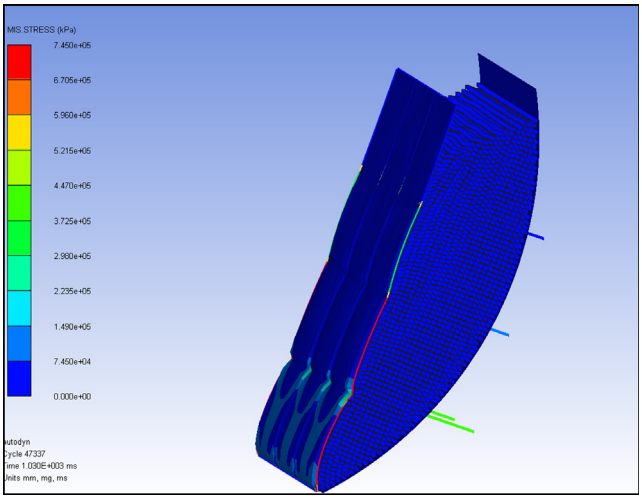

Fig. 27. General overview of deformation and Von Mises Stress. Case A.

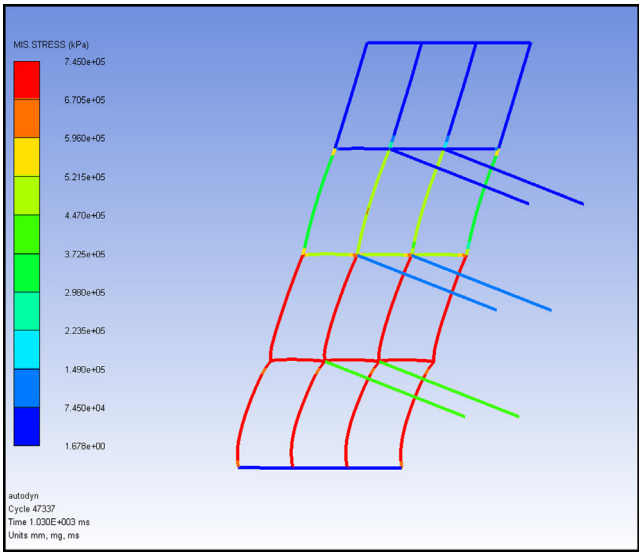

Fig. 28. Cables and bolts: Von Mises stress. Case A.

by means of decreasing the frictional coefficient between the wedge of unstable soil with the soil surface slide. As the frictional angle to be used is the residual once the free-falling of the soil begins, frictional coefficient is taken as tg (Φres), where Φres = Φpeak-2°.

Results obtained in the numerical modelling are shown in Section 6.3 below.

6.2. Combined densities on the soil

The wedge is imported from ANSYS as a solid, converted to SPH formulation through AUTODYN interface. SPH particles are specified through the sand material previously defined, with an element size appropriate (100 mm) for this model in order to improve the computational cost of the model.

Other issue that has been faced is the case of combined densities. In Cases C and D the slope presents an intermediate phreatic water level that goes through the soil wedge. This means that two different soil densities (saturated/submerged and dry density) are present, so two different SPH soil volumes will be the ideal solution. This approach is not possible for the Autodyn version employed in these calculations, as this software only allows to model a SPH volume per model (Fig. 25). The solution chosen is to employ a weighed density for the full wedge, depending on the volume percentage that each different density represents (Fig. 26).

In Case C, dry density of soil is 1.836 g/cm^3. The weighed density for this case is calculated as follows, obtaining the volumes of the different wedges from the geometry designer of Ansys and using for this case the submerged density of the soil (1.019 g/cm^3):

- Dry volume, d_d = 3.367e8 cm^3
- Below phreatic level volume, d_p = 3.166e8 cm^3
- Percentage of dry volume over the total, W_1 = 0.484
- Weighed density = $d_d \cdot W_1 + d_p \cdot W_2$ = 1.019 g/cm^3 ·0.484 + 1.83 6 g/cm^3 · (1–0.484) = 1.440 g/cm^3

Case D has a different weighed density as in the previous model, due to the density below the phreatic level is now saturated (2.03 g/cm^3). Following the same procedure:

Weighed density $= d_d W_1 + d_p W_2 = 2.03\ \text{g/cm}^3 \cdot 0.484 + 1.836\ \text{g/cm}^3 \cdot (1 - 0.484) = 1.929\ \text{g/cm}^3$

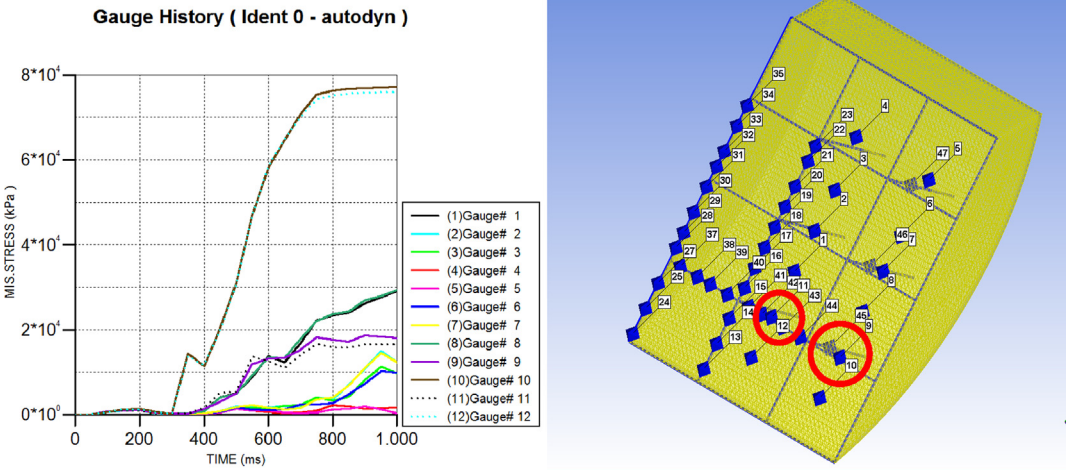

Fig. 29. Left: Von Mises stress vs. time of the membrane. Right: Location of all the gauge points. Case A.

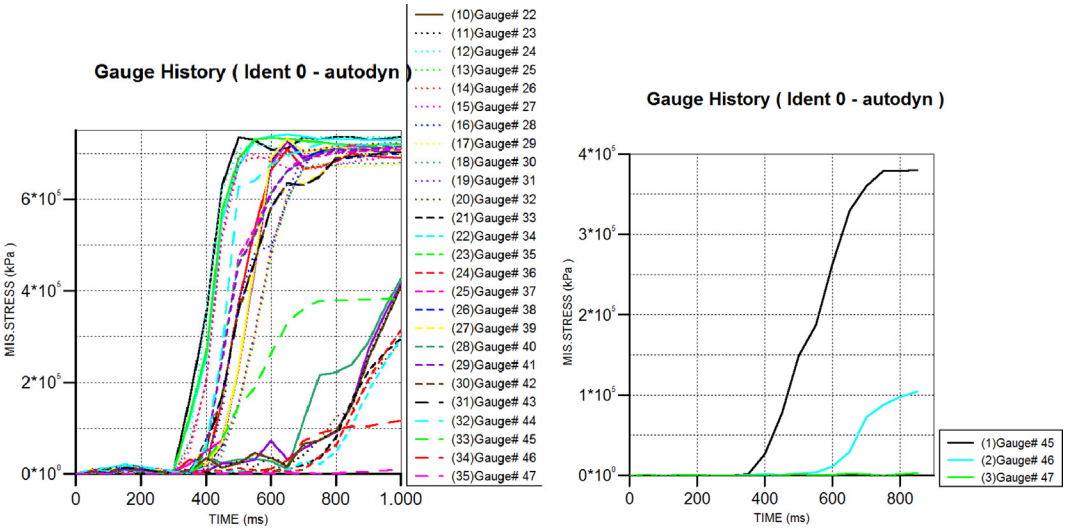

Fig. 30. Cables (left graph) and bolts (right graph) Von Mises stress vs. time for Case A.

6.3. Results of cylindrical case studies

Table 7 sums up the main properties of the four case studies selected, and results obtained are summarized in the Section 8 of this paper as conclusions.

6.3.1. Case A

First case study is simulated, stopping the calculation process as there are few elements of the flexible system that have reached the Von Mises stress. As it can be seen in Fig. 27, cables reach the Von Mises stress prior to the stabilisation of the soil falling once it is retained by the flexible system.

Isolating the view to the cables and bolts, the yield stress reached in cables of the lowest zone of the flexible system (745 MPa) is shown (Fig. 28).

In order to obtain the peak stresses at the membrane, gauge points that have been defined prior to the calculations can plot Von Mises stress vs. time. The position of these are shown in Fig. 29, and these positions have been placed according to the knowledge obtained from previous models as these are the points where peak stresses are foreseen. Plotted on the side is the graph obtained of the Von Mises stress during the free-falling simulation, where it can be checked at the gauge points 10 and 12 that the peak stress obtained is 77 MPa, the biggest value obtained.

Cables reach the yield stress at around 500 ms, redistributing the stresses over the other cables of the model until stabilisation (Fig. 30).

6.3.2. Case B

In this case (Fig. 31)the saturated density of the soil is employed, and from the results obtained in the last model more gauge points are placed along the cables in order to obtain the Von Mises stress graph along time. To make the behaviour of any of the elements present more comprehensible, gauge points are placed at the bolts as well.

Plotted in Figs. 32 and 33 are the gauge points graphs of the evolution of Von Mises stress against time for the structural elements of the flexible system. It is noted that in this model, the Von Mises peak stress value is reached in around 1000 ms, so it can be stated that when density of soil is bigger a major frictional force between soil wedge and sliding surface is developed. Thus, the impact against the flexible system is slower than in the previous case analysed, when peak stress was reached around 700 ms.

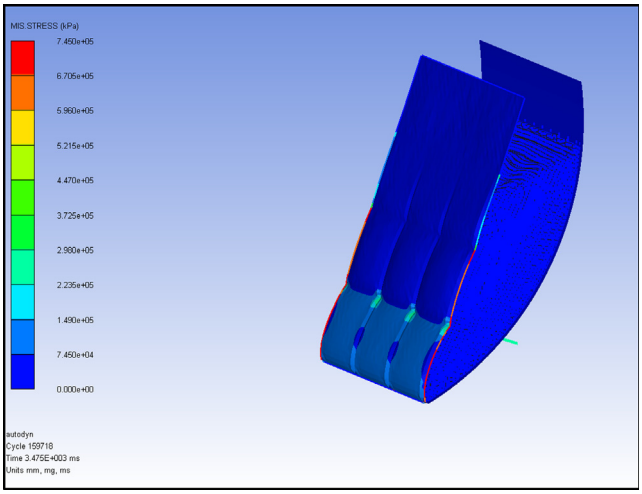

Fig. 31. General overview of deformation and Von Mises stress on Case B.

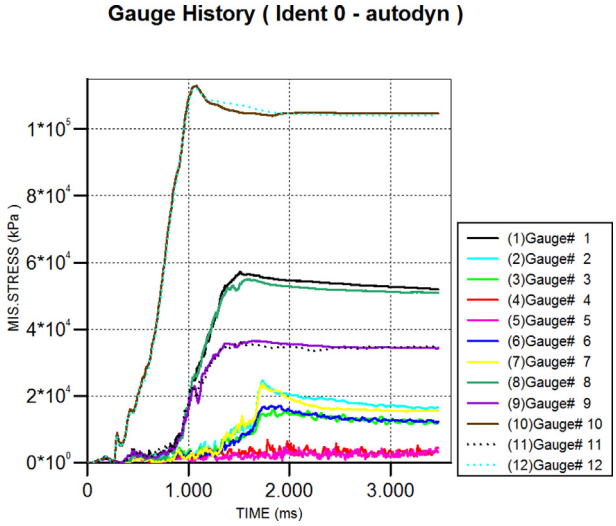

Fig. 32. Von Mises stress vs. time of the membrane for Case B.

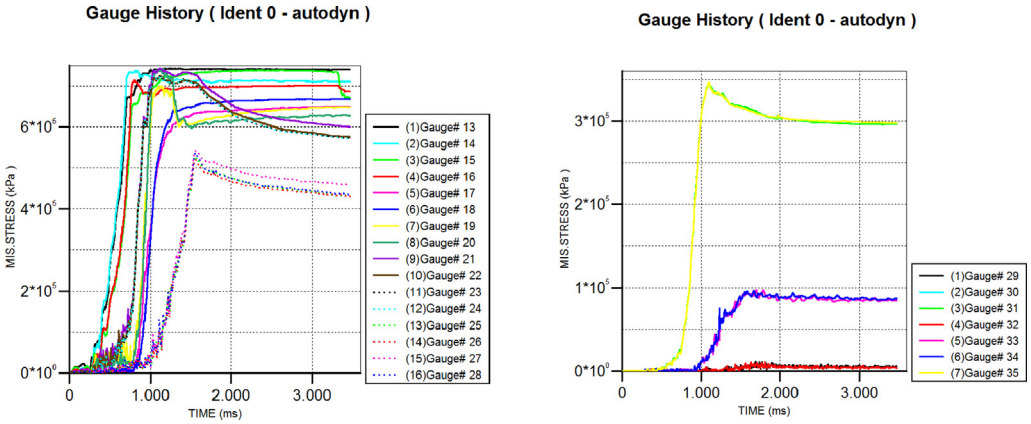

Fig. 33. Von Mises stress vs. time on the cables (left) and bolts (right) for Case B.

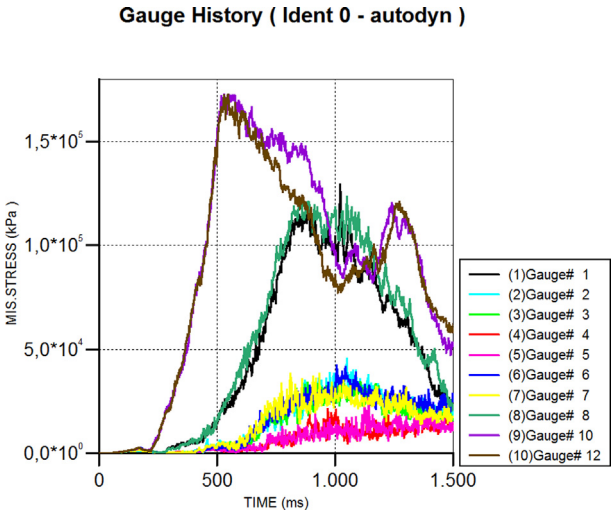

Fig. 34. Von Mises stress vs. time for gauge points on the membrane for Case C.

Despite the slower velocity impact happening due to the increase of density of the soil, this is going to develop bigger stress due once it is retained due to bigger weight of mass being contained. For this case, 130 MPa is reached at the peak moment (80 MPa in the first model).

The Von Mises stress evolution for cables and bolts can be seen in Fig. 33, thanks to the use of additional gauges on the model. Through the analysis of these graphs, cables reach the yield stress. This is happening for both vertical and horizontal cables. Bolt stresses are analysed as well, obtaining that their peak stress is much below their Von Mises stress (500 MPa; the two bottom bolts reach less than 400 MPa).

6.3.3. Case C

In this case, the slope presents a phreatic water level intermediate that goes through the soil wedge. The solution chosen, as stated previously in Section 6.2, is to employ a weighed density for the full wedge (see Fig. 34).

Results of Von Mises stress on the membrane can be seen on Fig. 34. From the previous models, cables of Ø16mm show not enough mechanical properties to adequately resist the stresses developed in the model without plastification. Therefore, new cables with Ø22mm were included in this case, updating the mechanical properties in the model.

Results obtained after calculations show that again, cables cannot avoid reaching the yield stress (Fig. 35 left). Time employed to reach the peak stress is around 500 ms. The peak stresses obtained do not show a stake regarding the yielding limits (Fig. 35 right).

6.3.4. Case D

This model has a different weighed density than the previous model, due to the density below the phreatic level is now saturated (2.03 g/cm^3).

As an attempt to increase the strength of the system, a different commercial cable net is employed. This is designated as Cable net 150 and is added to the material table. Thickness of this net model is 1.15 mm, instead of 1 mm which was used with cable net 200.

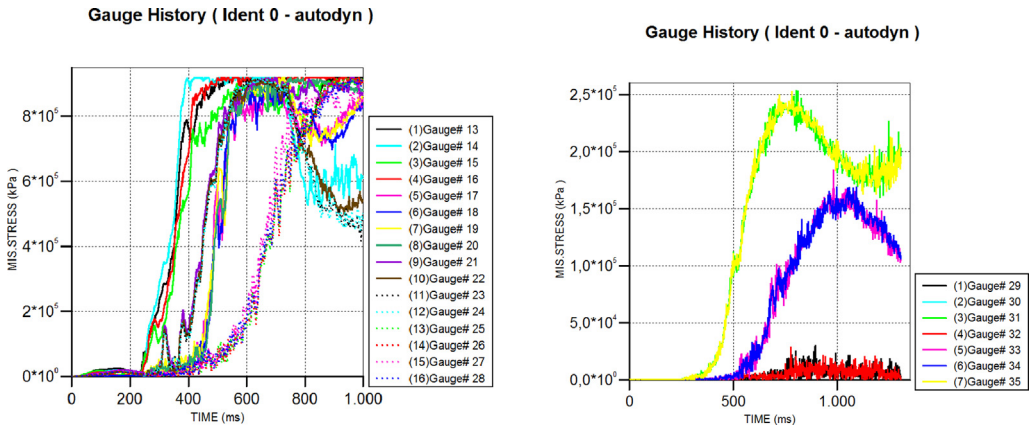

Fig. 35. Left: Von Mises stress vs. time for gauge points on the cables. Right: Von Mises stress vs. time for gauge points on the bolts. Case C.

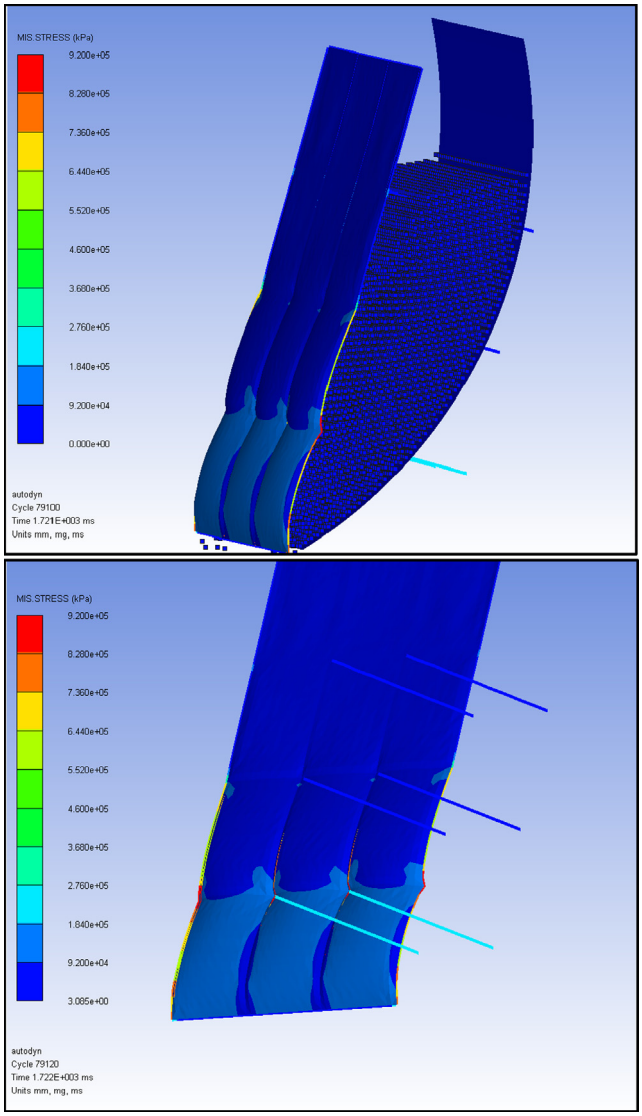

Fig. 36. Top: General isometric view of deformed model. Bottom: Cables + bolts + net deformation and Von Misses stress. Case D.

The objective is to try to avoid cables reaching the yield stress. Even with these assumptions, using more material on the flexible system, Von Mises stresses are reached again at the cables

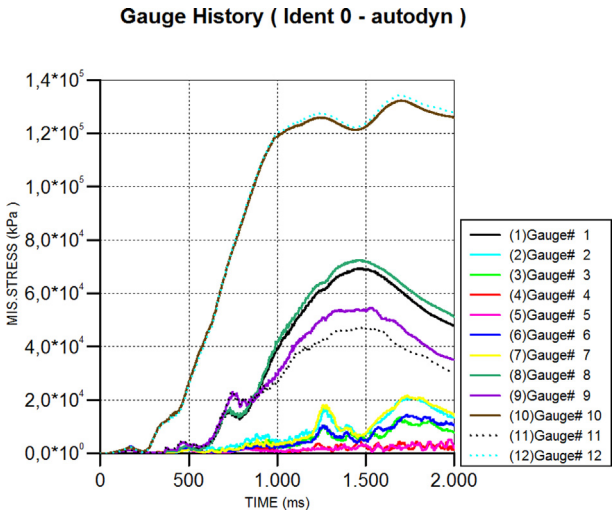

Fig. 37. Left: Von Mises stress vs. time at the membrane for Case D.

(Fig. 36 and Fig. 38 left). Results of Von Mises stress on the membrane can be seen on Fig. 37.

Once again, bolts do not present any yielding problem as these are always below 500 MPa, being the maximum 241 MPa (Fig. 38 right).

A table summary is presented below with the main results obtained, focusing on the peak stresses developed at each element of the flexible system (Table 8). The circular cases results are discarded in order to allow a good comparison between the behaviour of the different elements.

7. Model validation

In order to verify that the simulations correspond to a real response of a slope, a model validation is performed following the investigations made by Cala et al., 2013 [29]. The research work presented in this paper explains the verification of the existing dimensioning concept for superficial slope protection system based on test results coming from a large-scale field test setup. This system (Fig. 39) is going to be simulated using the criteria followed in the numerical modelling of this paper, so the results obtained from the simulations will be compared with the ones of the experimental test.

Materials employed are described in the paper and are summarized in Table 9. With regards to the soil characterisation, the same

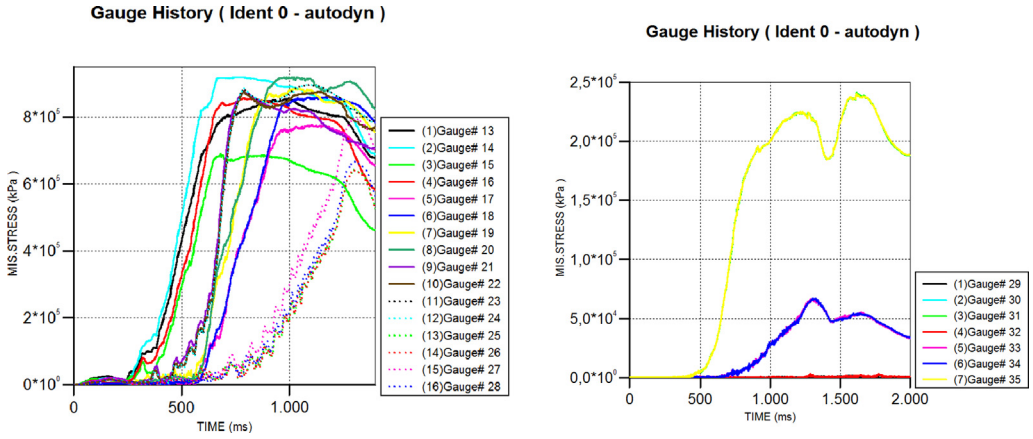

Fig. 38. Left: Von Mises stress vs. time at the cables, being 920 MPa the maximum. Right: Von Mises stress vs. time at the bolts. Case D.

Table 8
Summary of the results of each case study.

CASE	Wedge Soil	Cables	Anchorages	Membrane	Comments
CASE A					
Properties	μ_d = 0.44 d = 1.019 g/cm^3	Ø16mm σ_{yield} = 745 MPa	Ø28mm σ_{yield} = 500 MPa	Cable net 200 σ_{ult} = 155.9 MPa	
Von Mises peak stress		σ_{VM} = 745 MPa	σ_{VM} = 382 MPa	σ_{VM} = 77 MPa	Cables reach yield stress
CASE B					
Properties	μ_d = 0.44 d = 2.03 g/cm^3	Ø16mm σ_{yield} = 745 MPa	Ø28mm σ_{yield} = 500 MPa	Cable net 200 σ_{ult} = 155.9 MPa	
Von Mises peak stress		σ_{VM} = 745 MPa	σ_{VM} = 350 MPa	σ_{VM} = 130 MPa	Cables reach yield stress
CASE C					
Properties	μ_d = 0.67 d = 1.019 g/cm^3	Ø22mm σ_{yield} = 920 MPa	Ø28mm σ_{yield} = 500 MPa	Cable net 200 σ_{ult} = 155.9 MPa	
Von Mises peak stress		σ_{VM} = 920 MPa	σ_{VM} = 253 MPa	σ_{VM} = 168 MPa	Cables reach yield stress; flexible system reaches ultimate stress.
CASE D					
Properties	μ_d = 0.67 d = 1.836 g/cm^3	Ø22mm σ_{yield} = 920 MPa	Ø28mm σ_{yield} = 500 MPa	Cable net 150 σ_{ult} = 156.4 MPa	
Von Mises peak stress		σ_{VM} = 920 MPa	σ_{VM} = 241 MPa	σ_{VM} = 135 MPa	Cables reach yield stress.

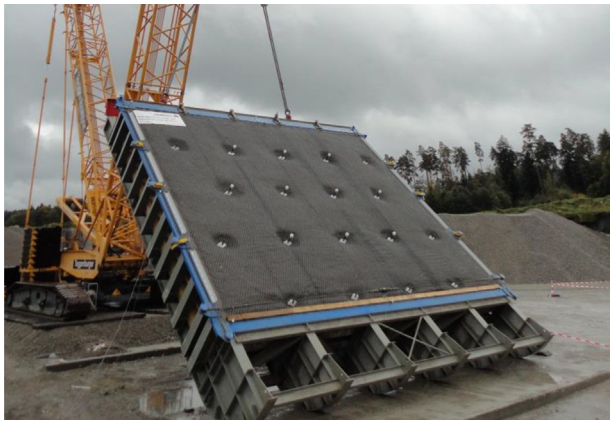

Fig. 39. Experimental setup for the flexible system (extracted from [29]).

considerations followed in this paper (related to curve data fit) are followed, as the only data available is the type of soil and density.

Geometry modelling follows the indications given in the large-scale test, and the steel box that is containing the soil is reproduced quite accurately. Anchorages are fixed on one end to the flexible membrane and fixed at the other end as well to the steel box (Fig. 40).

Box inclination angle is 85°, which is the configuration where the perpendicular displacement of the flexible system to the direction of the soil falling (gravity) is shown in [20].To achieve these measures, laser scanning techniques are employed. Results are shown in Figs. 41 and 42.

The maximum deformation of the membrane was measured on the numerical model by calculating the difference of the deformed (1756.3 mm) and original coordinates (1300 mm) in Z perpendicular to the inclination plane of the box, giving a value of 475.63 mm. The result obtained can be considered as a good result, due to the lack of an accurate table of material properties as well as

Table 9
Material properties employed in the numerical modelling from the real test.

	Density	EOS	Strength	Failure	Erosion
Flexible System – TECCO 65/3	3.30 g/cm3	Linear	Elastic	–	–
Soil – Recycling gravel	1.80 g/cm3	Linear - Compaction	MO Granular	Tensile Pressure	Geometric Strain
Cables – Ø22mm	7.85 g/cm3	Linear	Von Mises	–	–
Bolts - Ø28mm	7.85 g/cm3	Linear	Von Mises	–	–

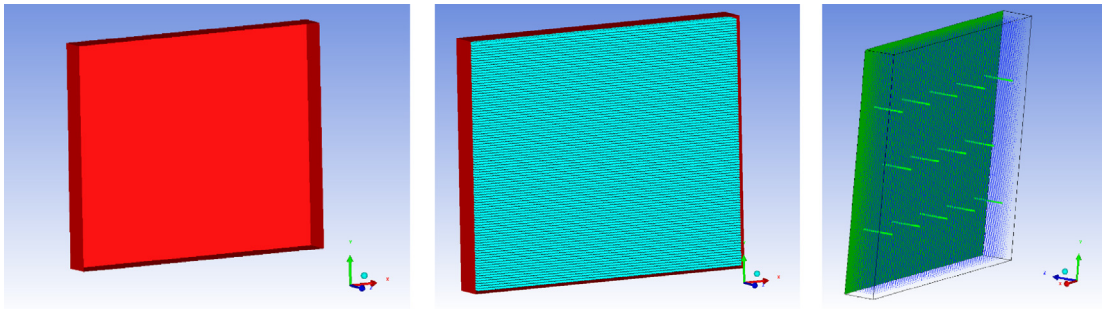

Fig. 40. Left: Geometry of the steel box. Centre: SPH particles to be contained inside the steel box. Right: Model with anchorages modelled.

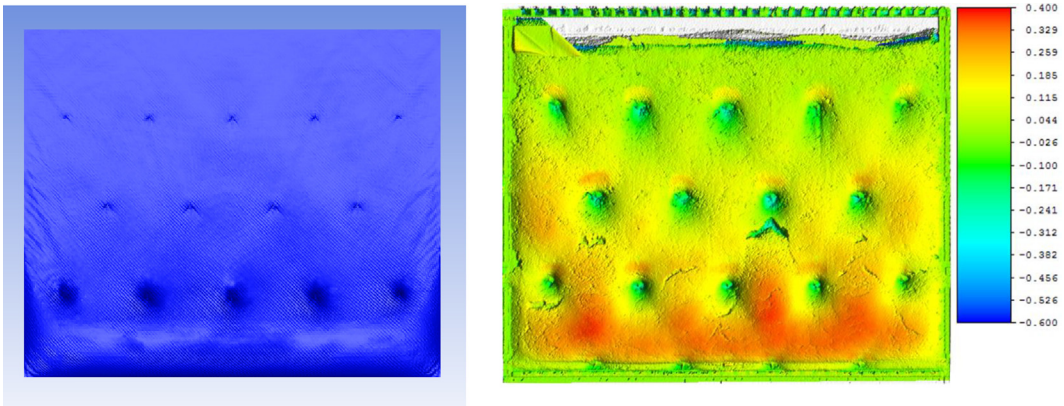

Fig. 41. Left: Deformation obtained with the numerical modelling. Right: Results obtained from real system with laser scanning extracted from [20], being the maximum 400 mm at the bottom side.

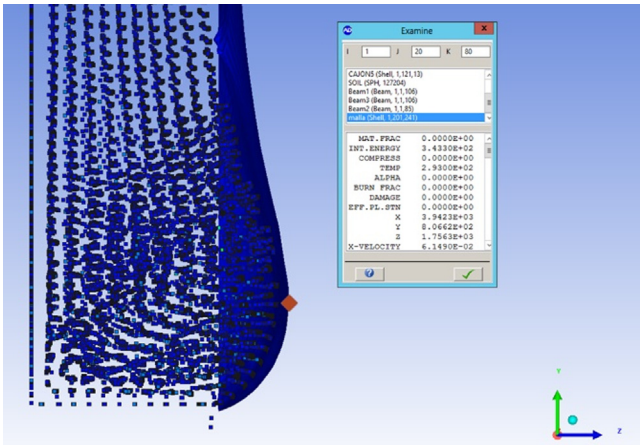

Fig. 42. Maximum displacement of the membrane on the red point.

a more precise laser scanner result. Once again, the numerical modelling here exposed shows a good approach to the physical phenomena under study, although it overestimates the deformation and therefore, the stresses on the membrane.

8. Conclusions

In this paper, an improvement of the numerical simulations that reproduce the behaviour of flexible systems anchored to the ground in a sliding event was developed. The change from 2D to 3D allowed the use of perimeter cables and intermediate bolts. Four cases from the 21 possible scenarios were analysed, differing in their geometry, phreatic level and soil type. The input of the different phreatic levels was approached by calculating a weighed density for all the SPH soil, since Autodyn does not allow creating two separate SPH regions with different properties. The membranes of the flexible system were simplified by using continuous shells with a certain thickness and resistance, instead of representing each cable of the squared reticle net. This allows a reduction of the implementation of the numerical model, besides a reduction of the computational time.

With the model validation included in Section 7, it is demonstrated that the model approach proposed in this paper is able to correctly reproduce the interaction of a soil sliding on a flexible system anchored to the ground, obtaining errors in displacement around 18% higher in the simulation than in the tests. This difference in the membrane deformation could be due to either the lack of knowledge of the material used on the experimental test simulated or to an excessively low friction angle (0.2) between the membrane and the soil.

From the four cases simulated, we can conclude that all of the cables reach their yield stress but none of them reached the ultimate stress. Only in Case C, the membrane breaks since it overpassed the ultimate stress, although for not a great amount. This could be due to the fact that the friction angle between membrane and soil was quite low as discussed previously.

The model built for AUTODYN could be useful for geotechnical designers in order to first estimate the needed section and material parameters for the cables, anchorages and membrane for the case designed. These models would require an experimental test check in order to see the real approach and accuracy when the flexible system is used under operating conditions and if calibration of some of the parameters of the model is necessary. As a criterion to accept/discard a flexible system design, reaching the yield stress once the sliding has happened is acceptable, but not if the flexible system breaks. From the results obtained and summarized on Table 8, only the Case planar D design should be accepted.

Further experimental investigation or studies could be useful regarding the interfaces of different elements, as for example, frictional coefficient of the unstable wedge of soil and the stable sliding surface, how it decays, how the wedge interacts with the membrane surface, or interface between SPH volumes of different material properties simulating different layers of terrain or water conditions.

The simulations made show the degree of importance of employing dynamic simulations in these geotechnical applications, due to if a static calculation is made the peak stresses that have been detected in these dynamic simulations are not detected so the design is at stake of being ineffective in case of slope sliding.

The different studies between employing saturated or submerged density have proven the importance of the presence of water or absence in the soil, as this is going to affect the magnitude of the impact of the flexible system.

Funding

The FORESEE project has received funding from the European Union's Horizon 2020 research and innovation program under grant agreement No 769373.

This scientific paper reflects only the author's views, and the Commission is not responsible for any use that may be made of the information contained therein.

Declaration of Competing Interest

The authors declare that they have no known competing financial interests or personal relationships that could have appeared to influence the work reported in this paper.

Acknowledgements

The authors would like to thank MallaTalud Cantabria (MTC) for supplying the cable nets, coconut fibre mesh and cables to be considered in this study, and LADICIM and LabEST from the University of Cantabria for testing them in their facilities.

References

[1] Shukla PR, Skea J, Calvo Buendia E, Masson-Delmotte V, Pörtner H-O, Roberts DC, et al. (Eds.), IPCC, 2019: Climate Change and Land: an IPCC special report on climate change, desertification, land degradation, sustainable land management, food security, and greenhouse gas fluxes in terrestrial ecosystems [in press].
[2] Sharma LK, Umrao RK, Singh R, Ahmad M, Singh TN. Geotechnical characterization of road cut hill slope forming unconsolidated geo-materials: a case study. Geotech Geol Eng 2017;35(1):503–15. doi: https://doi.org/10.1007/s10706-016-0093-8.
[3] Singh PK, Kainthola A, Panthee S, Singh TN. Rockfall analysis along transportation corridors in high hill slopes. Environ Earth Sci. 2016;75:441. doi: https://doi.org/10.1007/s12665-016-5489-5.
[4] Blanco-Fernandez E, Castro-Fresno D, Díaz JJDC, Lopez-Quijada L. Flexible systems anchored to the ground for slope stabilisation: Critical review of existing design methods. Eng Geol 2011;122(3–4):129–45. doi: https://doi.org/10.1016/j.enggeo.2011.05.014.
[5] Castanon-Jano L, Castro-Fresno D, Blanco-Fernandez E, Carpio-Garcia J. Selection of membranes and linking method in slope stabilization systems for the reduction on the installation time using multi-criteria decision analysis. Ain Shams Eng J 2021. doi: https://doi.org/10.1016/j.asej.2021.03.010.
[6] Castanon-Jano L, Blanco-Fernandez E, Castro-Fresno D, Ferreño D. Use of explicit FEM models for the structural and parametrical analysis of rockfall protection barriers. Eng Struct 2018;166:212–26. doi: https://doi.org/10.1016/j.engstruct.2018.03.064.
[7] Blanco-Fernandez E, Castro-Fresno D, del Coz Diaz JJ, Navarro-Manso A, Alonso-Martinez M. Flexible membranes anchored to the ground for slope stabilisation: Numerical modelling of soil slopes using SPH. Comput Geotech 2016;78:1–10. doi: https://doi.org/10.1016/j.compgeo.2016.04.014.
[8] Escallón JP, Wendeler C, Chatzi E, Bartelt P. Parameter identification of rockfall protection barrier components through an inverse formulation. Eng Struct 2014;77:1–16. doi: https://doi.org/10.1016/j.engstruct.2014.07.019.
[9] Qiao S, Xu P, Teng J, Sun X. Numerical Study of Optimal Parameters on the High Filling Embankment Landslide Reinforced by the Portal Anti-Slide Pile. KSCE J Civ Eng 2020;24(5):1460–75. doi: https://doi.org/10.1007/s12205-020-1743-1.
[10] Ghosh B, Fatahi B, Khabbaz H, Nguyen HH, Kelly R. Field study and numerical modelling for a road embankment built on soft soil improved with concrete injected columns and geosynthetics reinforced platform. Geotext Geomembranes 2021;49(3):804–24. doi: https://doi.org/10.1016/j.geotexmem.2020.12.010.
[11] Johari A, Hajivand AK, Binesh SM. System reliability analysis of soil nail wall using random finite element method. Bull Eng Geol Environ 2020;79 (6):2777–98. doi: https://doi.org/10.1007/s10064-020-01740-y.
[12] Johari A, Kalantari AR. System reliability analysis of soldier-piled excavation in unsaturated soil by combining random finite element and sequential compounding methods. Bull Eng Geol Environ 2021;80(3):2485–507. doi: https://doi.org/10.1007/s10064-020-02022-3.
[13] Gholampour A, Johari A. Reliability-based analysis of braced excavation in unsaturated soils considering conditional spatial variability. Comput Geotech 2019;115:103163. doi: https://doi.org/10.1016/j.compgeo.2019.103163.
[14] Johari A, Talebi A. Stochastic analysis of rainfall-induced slope instability and steady-state seepage flow using random finite-element method. Int J Geomech 2019;19(8):04019085. doi: https://doi.org/10.1061/(ASCE)GM.1943-5622.0001455.
[15] Kainthola A, Singh PK, Wasnik AB, Sazid M, Singh TN. Finite element analysis of road cut slopes using Hoek and Brown failure criterion. Int J Earth Sci Eng 2012;5(5):1100–9.
[16] Mahanta B, Singh HO, Singh PK, Kainthola A, Singh TN. Stability analysis of potential failure zones along NH-305. India. Nat Hazards 2016;83:1341–57. doi: https://doi.org/10.1007/s11069-016-2396-8.
[17] Sasiharan N, Muhunthan B, Badger TC, Shu S, Carradine DM. Numerical analysis of the performance of wire mesh and cable net rockfall protection systems. Eng Geol 2006;88(1–2):121–32. doi: https://doi.org/10.1016/j.enggeo.2006.09.005.
[18] Bui HH, Fukagawa R, Sako K, Ohno S. Lagrangian meshfree particles method (SPH) for large deformation and failure flows of geomaterial using elasticplastic soil constitutive model. Int J Numer Anal Meth Geomech 2008;32(12):1537–70. doi: https://doi.org/10.1002/nag.v32:1210.1002/nag.688.
[19] Li L, Zhai M, Ling X, Chu X, Hu B, Cheng Y. On the Location of Multiple Failure Slip Surfaces in Slope Stability Problems Using the Meshless SPH Algorithm. Advances in Civil Engineering 2020;2020:1–8. doi: https://doi.org/10.1155/2020/6821548.
[20] Yu M, Huang Y, Deng W, Cheng H. Forecasting landslide mobility using an SPH model and ring shear strength tests: A case study. Nat Hazard Earth Sys 2018;18(12):3343–53. doi: https://doi.org/10.5194/nhess-18-3343-2018.
[21] DYWIDAG. Gama de Productos Geotécnicos DYWIDAG; 2021:04170-3/07.14-2.000 ka mm [in Spanish].
[22] Castro-Fresno D, Coz Diaz JJ, López LA, García Nieto PJ. Evaluation of the resistant capacity of cable nets using the finite element method and experimental validation. Eng Geol 2008;100(1–2):1–10. doi: https://doi.org/10.1016/j.enggeo.2008.02.007.
[23] Bui HH, Fukagawa R, Sako K, Wells JC. Slope stability analysis and discontinuous slope failure simulation by elasto-plastic smoothed particle hydrodynamics (SPH). Geotechnique 2011;61(7):565–74. doi: https://doi.org/10.1680/geot.9.P.046.
[24] Nonoyama H, Moriguchi S, Sawada K, Yashima A. Slope stability analysis using smoothed particle hydrodynamics (SPH) method. Soils Found 2015;55 (2):458–70. doi: https://doi.org/10.1016/j.sandf.2015.02.019.
[25] Laine L, Larsen O. Proposal on How to Model the Unloading in a Compaction Equation of State based upon Tri-axial tests on Dry Sand; 2010.
[26] Laine L, Sandvik A. Derivation Of Mechanical Properties For Sand; 2001.
[27] Nogueira CG, Rodrigues ID. Ductility Analysis of RC Beams Considering the Concrete Confinement Effect Produced by the Shear Reinforcement: a Numerical Approach. Lat Am J Solids Stru 2017;14(13):2342–72. doi: https://doi.org/10.1590/1679-78253904.
[28] Muhunthan B, Shu S, Sasiharan N, Hattamleh O A, Badger TC, Lowell SM, et al. Analysis and design of wire mesh/cable net slope protection. Rep. No. WA-RD 612.1. Seattle, Washington, USA: Washington State Transportation Center (TRAC); 2005.
[29] Cala M, Stolz M, Baraniak P, Rist A, Roduner A. Large Scale Field Tests for Slope Stabilizations Made with Flexible Facings. Paper presented at the ISRM International Symposium - EUROCK 2013, Wroclaw, Poland, October 2013, 2013.

Jose Carlos Jimenez Fernandez University degree (Bach) in Civil Engineering in the University of Burgos, Spain, and postgraduate with a MSc in Finite Element Analysis in University of Madrid, Spain. Specialized in the design and analysis with FEA, focused in nonlinear and dynamic analysis. In Tecnalia, involved in Structural Health Monitoring projects of civil structures, apart from other research and development projects related to Civil Engineering. Experience with experimental modal analysis of structures, post processing the information measured in the structure and calibrating FE models with the information obtained from the measuring campaign.

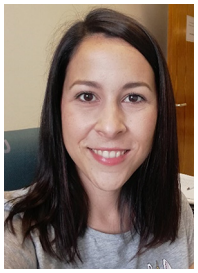

Laura Castanon-Jano Laura Castañón Jano holds a degree in Industrial Engineering at the University of Oviedo and a PhD. on Civil Engineering at the University of Cantabria.
Her research topics are related to slope protection systems, behavior of concrete and additive manufacturing. She has published 6 scientific papers, is coauthor of an international patent and collaborated in 9 research projects. She also attended to 4 national and international conferences and made an international 3 month stay at Imperial College London.
Currently she has a post of Assistant Lecturer on the Area of Manufacturing Engineering.

Alvaro Gaute Alonso Civil Engineer by the University of Cantabria and PhD in 2017. Currently, associate professor of Structural Engineering and member of the research group on Instrumentation and Dynamic Analysis of Structures at the University of Cantabria. Specialist in Monitoring and Characterization of Civil Engineering structures, he has participated in numerous international impact projects.

Elena Blanco-Fernandez Elena Blanco Fernandez holds a degree of civil engineering and a PhD. at the University of Cantabria. She currently has a post of Associate Professor and she is involved in modules related with project management, sustainable construction, research methods, geosynthetics and flexible systems for slope protection. She has published 18 scientific papers related to these topics.
Remark, as well, that she is currently the co-responsible of the European research project 3DPARE. She's been the responsible of the research contract with the Chilean company Inchalam, S.L. for the 'Developing of a dynamic barrier against rockfalls', as well as of the research contract 'Octopus' that consist on the development of a new monitoring system of slopes protected with flexible systems.
She is the Technical Director of the Geosynthetics Laboratory of the Universidad de Cantabria (LAGUC), and holds the position of Sub-Head of the Department of Transportation and Technology or Projects and Process.

Juan Carlos Gonzalez Juan Carlos Gonzalez holds a degree in geology at the University of Oviedo (MSc in Geological Sciences-EQF-7).
Over 25 years' experience in geotechnical and underground works, including stability of slopes, tunneling, foundations and ground improvement, in all phases of work, from the site investigation to the design of technical solutions. He is regularly involved in slope stability analysis in soils and rocks, as well as in the geological study for foundations and tunnels.
He is currently developing, in WSP-Spain, the design and supervision of reinforcement and stabilization of slopes in several project in Spain, Sweden, Chile and Colombia.

Victor Centeno Gonzalez MSc Civil Engineering & University Expert in Professional Construction for the University of Cantabria (Spain), Project Manager Professional (PMP®) and awards price for the best final Degree Project. Has over 6 years' experience on detailed design & supervision of project in the Cost, Operation and Maintenance department of WSP Spain – Apia. He has participated in numerous international projects of roads, railways and airports, in pavements, cost, specifications and maintenance areas. Also, he has participated in research projects like climate risk management tools for roads and airports.

Daniel Castro-Fresno Civil Engineer by the University of Cantabria and PhD in 2001, awarded the ANCI prize to PhD theses. Currently, Full Professor of Construction Engineering, Director of the Dept. of Transports, and Manager of the Construction Technology Applied Research Group (GITECO) of the University of Cantabria. Supervisor of 25 PhD theses, 18 of which in the last 10 years, highlighting in 2012 the thesis by Elena Blanco, "Flexible Systems of High Resistance for Stabilisation of Slopes. Revision of the current methods and proposal of new methodology", awarded by the ANCI prize to PhD theses. Co-author of 153 indexed papers in JCR, collaborating as reviewer in several international scientific journals. Co-author of more than 100 presentations in national and international congresses, has 27 patents, 10 international, together with 2 protected software.

David Garcia-Sanchez Mr. David Garcia-Sanchez, (male), MSc Civil Engineering and PhD Structural and Mechanical Engineering at University of Cantabria, Spain. Has over 10 years' experience on bridges and structures design, structural health monitoring and bridge inspection, civil engineering and offshore projects in Louis Berger International Design Center (a WSP Company). Since 2016 Senior Researcher and Knowledge Leader in the Infrastructures Area of Tecnalia (Basque Research Technology Alliance member) participating in several national and international research projects. He has co-Directed several Master Thesis at University of Cantabria. Currently, co-Directing one PhD Thesis at UPV/EHU. Member of ACHE, the Spanish Scientific-Technical Association of Structural Concrete and AEND, the Non Destructive Testing Spanish Association. Also IABMAS member (International Association for Bridges, Management and Safety). He is one international patent owner and two protected softwares. Honorary Lecturer of the Department of Structural and Mechanical Engineering at University of Cantabria (2010 and 2011). Co-author of 20 indexed papers in JCR, collaborating as reviewer in several international scientific journals. Co-author of more than 20 presentations in national and international congresses.